Search for a W' boson decaying to a vector-like quark and a top or bottom quark in the all-jets final state

CMS Collaboration ; Canelli, Maria Florencia ; Kilminster, Benjamin ; Aarrestad, Thea K ; Brzhechko, Danyyl ; Caminada, Lea ; de Cosa, Annapaoloa ; Del Burgo, Riccardo ; Donato, Silvio ; Galloni, Camilla ; Hreus, Tomas ; Leontsinis, Stefanos ; Mikuni, Vinicius Massami ; Neutelings, Izaak ; Rauco, Giorgia ; Robmann, Peter ; Salerno, Daniel ; Schweiger, Korbinian ; Seitz, Claudia ; Takahashi, Yuta ; Wertz, Sebastien ; Zucchetta, Alberto ; et al

Abstract: A search for a heavy W resonance decaying to one B or T vector-like quark and a top or bottom quark, respectively, is presented. The search uses proton-proton collision data collected in 2016 with the CMS detector at the LHC, corresponding to an integrated luminosity of 35.9 fb^1 at $\sqrt{s} = 13$ TeV. Both decay channels result in a final state with a top quark, a Higgs boson, and a b quark, each produced with significant energy. The all-hadronic decays of both the Higgs boson and the top quark are considered. The final-state jets, some of which correspond to merged decay products of a boosted top quark and a Higgs boson, are selected using jet substructure techniques, which help to suppress standard model backgrounds. A W boson signal would appear as a narrow peak in the invariant mass distribution of these jets. No significant deviation in data with respect to the standard model background predictions is observed. Cross section upper limits on W boson production in the top quark, Higgs boson, and b quark decay mode are set as a function of the W mass, for several vector-like quark mass hypotheses. These are the first limits for W boson production in this decay channel, and cover a range of 0.01 to 0.43 pb in the W mass range between 1.5 and 4.0 TeV.

DOI: https://doi.org/10.1007/JHEP03(2019)127

Zucchetta, Alberto; et al (2019). Search for a W' boson decaying to a vector-like quark and a top or bottom quark in the all-jets final state. Journal of High Energy Physics, 03:127.
DOI: https://doi.org/10.1007/JHEP03(2019)127

Published for SISSA by Springer

Received: November 16, 2018
Accepted: March 1, 2019
Published: March 22, 2019

Search for a W′ boson decaying to a vector-like quark and a top or bottom quark in the all-jets final state

The CMS collaboration

E-mail: cms-publication-committee-chair@cern.ch

Abstract: A search for a heavy W′ resonance decaying to one B or T vector-like quark and a top or bottom quark, respectively, is presented. The search uses proton-proton collision data collected in 2016 with the CMS detector at the LHC, corresponding to an integrated luminosity of 35.9 fb^{-1} at $\sqrt{s} = 13$ TeV. Both decay channels result in a final state with a top quark, a Higgs boson, and a b quark, each produced with significant energy. The all-hadronic decays of both the Higgs boson and the top quark are considered. The final-state jets, some of which correspond to merged decay products of a boosted top quark and a Higgs boson, are selected using jet substructure techniques, which help to suppress standard model backgrounds. A W′ boson signal would appear as a narrow peak in the invariant mass distribution of these jets. No significant deviation in data with respect to the standard model background predictions is observed. Cross section upper limits on W′ boson production in the top quark, Higgs boson, and b quark decay mode are set as a function of the W′ mass, for several vector-like quark mass hypotheses. These are the first limits for W′ boson production in this decay channel, and cover a range of 0.01 to 0.43 pb in the W′ mass range between 1.5 and 4.0 TeV.

Keywords: Beyond Standard Model, Hadron-Hadron scattering (experiments), vector-like quarks

ArXiv ePrint: 1811.07010

https://doi.org/10.1007/JHEP03(2019)127

JHEP03(2019)127

Contents

JHEP03(2019)127

1 Introduction

Many extensions of the standard model (SM) predict new massive charged gauge bosons [1–3]. The W′ boson is a hypothetical heavy partner of the SM W gauge boson that could be produced in proton-proton (pp) collisions at the CERN LHC. Searches for W′ bosons have been most recently performed at a center-of-mass energy of 13 TeV by the CMS and ATLAS Collaborations in the lepton-neutrino [4, 5], diboson [6, 7], and diquark [8, 9] final states. Vector-like quarks (VLQs) are hypothetical heavy partners of SM quarks for which the left- and right-handed chiralities transform the same way under SM gauge groups. Searches for VLQs have been performed by the CMS and ATLAS Collaborations in both the single [10–13] and pair production [14–16] channels. The decay of the W′ boson to a heavy B or T VLQ and a top or b quark, respectively, is predicted, e.g., in composite Higgs boson models with custodial symmetry protection [17–19]. These models stabilize the quantum corrections to the Higgs mass and preserve naturalness. The W′ branching fraction to a quark and a VLQ depends on the VLQ mass, with a maximum of 50% in the high VLQ mass range at the threshold of custodian production (see ref. [20]).

A search for a W′ boson in this decay mode is presented for the first time. The analysis considers the decay channel where the B or T VLQ decays into a Higgs boson and a b or

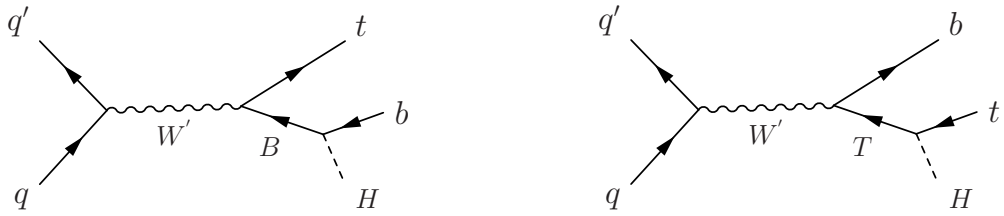

Figure 1. The W′ boson production and decays considered in the analysis. The analysis assumes equal branching fractions for W′ boson to tB and bT and 50% for each VLQ to qH.

top quark, respectively, in the all-jets final state. Both the B and T VLQ-mediated decays result in the same signature, as can be seen in figure 1. Because of the high W′ and VLQ masses considered in this analysis, the decay products are highly Lorentz boosted. These boosted decay products are reconstructed as single jets with distinct substructure, which is used in the analysis to distinguish them from SM multijet production. An inclusive search for a W′ boson decaying to a top quark, a Higgs boson, and a b quark is performed. The SM background is dominated by events comprised of jets produced via the strong interaction, referred to as quantum chromodynamics (QCD) multijet events, and top quark pair production ($\mathrm{t\bar{t}}$) events. These backgrounds are modeled by a combination of Monte Carlo (MC) simulation and control regions in data. The invariant mass distribution of the three-jet system, m_{tHb}, is used to set the first limits on the W′ boson production cross section in the decay channel to a B or T VLQ. The data sample used in the analysis corresponds to an integrated luminosity of $35.9\,\mathrm{fb}^{-1}$ [21] of pp collision data at $\sqrt{s} = 13\,\mathrm{TeV}$, recorded in 2016.

The theoretical framework followed in the analysis is described in ref. [20]. In this model the top and W′ are superpositions of elementary and composite modes, with the top degree of compositeness given by s_{L}, and the mixing angle of the elementary and composite W′ states given by θ_2. The W′ boson production cross section is inversely proportional to $\cot^2(\theta_2)$, but low $\cot(\theta_2)$ values tend to be dominated by the leptonic W′ boson decay mode. High values of the s_{L} parameter increase the relative phase space for the decay into two VLQs, whereas low s_{L} values enhance the W′ diboson decays. The analysis assumes this theoretical framework as evaluated at $s_{\mathrm{L}} = 0.5$ and $\cot(\theta_2) = 3$, which is chosen for the purposes of sensitivity in the W′ decay channel to a single VLQ. The expected signal cross sections in the analysis are evaluated at 13 TeV using the framework of ref. [20] for W′ masses in the range 1.5 to 4.0 TeV with the assumptions that the W′ →VLQ branching fraction is equally distributed between the tB and bT final states. As a benchmark for the analysis, the VLQ branching fractions for each of the decays B →bH and T →tH are assumed to be 50%, consistent with the benchmark used in other recent searches.

2 The CMS detector

The central feature of the CMS apparatus is a superconducting solenoid of 6 m internal diameter, providing a magnetic field of 3.8 T. Within the solenoid volume are a silicon pixel and strip tracker, a lead tungstate crystal electromagnetic calorimeter (ECAL), and

JHEP03(2019)127

a brass and scintillator hadron calorimeter (HCAL), each composed of a barrel and two endcap sections. Forward calorimeters extend the pseudorapidity coverage provided by the barrel and endcap detectors. Muons are detected in gas-ionization chambers embedded in the steel flux-return yoke outside the solenoid. A more detailed description of the CMS detector, together with a definition of the coordinate system used and the relevant kinematic variables, can be found in ref. [22].

The particle-flow algorithm [23] aims to reconstruct and identify each individual particle with an optimized combination of information from the various elements of the CMS detector. The energy of each photon is obtained from the ECAL measurement. The energy of each electron is determined from a combination of the electron momentum at the primary interaction vertex as determined by the tracker, the energy of the corresponding ECAL cluster, and the energy sum of all bremsstrahlung photons spatially compatible with originating from the electron track. The energy of each muon is obtained from the momentum, which is measured by the curvature of the corresponding track. The energy of each charged hadron is determined from a combination of their momentum measured in the tracker and the matching ECAL and HCAL energy deposits, corrected for zero-suppression effects and for the response function of the calorimeters to hadronic showers. Finally, the energy of each neutral hadron is obtained from the corresponding corrected ECAL and HCAL energies that are not associated with a charged hadron track.

Jets are clustered with the anti-k_{T} [24] algorithm in the FastJet 3.0 [25] software package. Jet momentum is determined as the vectorial sum of all particle momenta in the jet, and is found from simulation to be within 5 to 10% of the true momentum over the whole p_{T} spectrum and detector acceptance. Additional pp interactions within the same or nearby bunch crossings (pileup) can contribute additional tracks and calorimetric energy depositions to the jet momentum. To mitigate this effect, charged particles originating from sub-leading pp collision vertices within the same or adjacent bunch crossings are discarded in the jet clustering procedure, where the primary collision vertex is defined as the vertex largest quadrature-summed p_{T} of all reconstructed particles. To account for the neutral pileup component, the pileup per particle identification (PUPPI) algorithm [26] is used, which applies weights that rescale the jet transverse momentum based on the per-particle probability of originating from the primary vertex prior to jet clustering. Jet energy corrections are derived from simulation studies so that the average measured response of jets becomes identical to that of particle level jets. In situ measurements of the momentum balance in dijet, photon+jet, Z+jet, and multijet events are used to determine any residual differences between the jet energy scale in data and in simulation, and appropriate corrections are made [27]. Additional selection criteria are applied to each jet to remove jets potentially dominated by instrumental effects or reconstruction failures. The jet energy resolution amounts typically to 15% at 10 GeV, 8% at 100 GeV, and 4% at 1 TeV, to be compared to about 40, 12, and 5% obtained when the calorimeters alone are used for jet clustering.

Events of interest are selected using a two-tiered trigger system [28]. The first level (L1), composed of custom hardware processors, uses information from the calorimeters and muon detectors to select events at a rate of around 100 kHz within a time interval of less

JHEP03(2019)127

than 4 μs. The second level, known as the high-level trigger (HLT), consists of a farm of processors running a version of the full event reconstruction software optimized for fast processing, and reduces the event rate to around 1 kHz before data storage.

3 Simulated samples

The $\mathrm{t\bar{t}}$ production background is estimated from simulation, and is generated with POWHEG 2.0 [29–32]. The signal samples are generated at leading order using MadGraph5_aMC@NLO 2.3.3 [33, 34] with the NNPDF3.0 leading order parton distribution function (PDF) set, in the mass range from 1.5 to 4.0 TeV in 0.5 TeV increments. The analysis uses a QCD multijet sample as a cross check for the background estimate, which is also generated at LO with MadGraph5_aMC@NLO. Parton showering and hadronization are simulated with PYTHIA8.212 [35] using either the CUETP8M2T4 [36] or CUETP8M1 [37] underlying event tunes. For each $\mathrm{W'}$ boson mass point, three VLQ mass points are generated with the VLQ mass range from 0.8 to 3.0 TeV. The generated VLQ masses are scaled to the $\mathrm{W'}$ boson mass ($m_{\mathrm{W'}}$) such that there is a low ($\approx 1/2m_{\mathrm{W'}}$), medium ($\approx 2/3m_{\mathrm{W'}}$), and high ($\approx 3/4m_{\mathrm{W'}}$) mass sample for each $\mathrm{W'}$ boson mass point in order to explore the sensitive phase space of the boosted $\mathrm{W'}$ boson decay products. The generated $\mathrm{W'}$ boson and VLQ widths are narrow as compared with the detector and reconstruction resolutions which is in accord with theoretical predictions for most of the analyzed phase space. The simulation of the CMS detector uses Geant4 [38]. All MC samples include pileup simulation and are weighted such that the distribution of the number of interactions per bunch crossing agrees with that observed in data.

4 Event reconstruction

The $\mathrm{W'} \to \mathrm{T/B} \to \mathrm{tHb}$ channel is characterized by three high-p_{T} jets. The jets from the top quark (top jet) and Higgs boson (Higgs jet) decays tend to be wide and massive, whereas the jet from the b quark (b jet) will tend to be narrow and have a lower mass. Therefore, one jet clustered with the anti-k_{T} algorithm with a distance parameter of 0.8 (AK8 jet) with $p_{\mathrm{T}} > 300$ GeV is required for the Higgs boson candidate jet. One AK8 jet with $p_{\mathrm{T}} > 400$ GeV is required for the top quark candidate jet. One anti-k_{T} jet with a distance parameter of 0.4 (AK4 jet) with $p_{\mathrm{T}} > 200$ GeV is required for the b candidate jet. The separation $\Delta\mathrm{R}$ ($\sqrt{(\Delta\phi)^2 + (\Delta\eta)^2}$) between the two AK8 jets is required to be at least 1.8 in order to reduce the correlation of jet shapes arising from the abutting of jet boundaries, which can bias the background estimate. The AK8 jets are then selected as being consistent with a top quark or a Higgs boson decay using the tagging procedures defined below. The collection of jets considered for the b quark candidate is then populated by AK4 jets with $\Delta\mathrm{R}$ of at least 1.2 from the tagged AK8 jets. In the case of multiple jets with the same tag, the tagged candidate is chosen randomly. Jet identification criteria are used for these three jets in order to reduce the impact of spurious jets from detector noise [39]. All jets in the analysis are required to be within $|\eta| < 2.4$.

JHEP03(2019)127

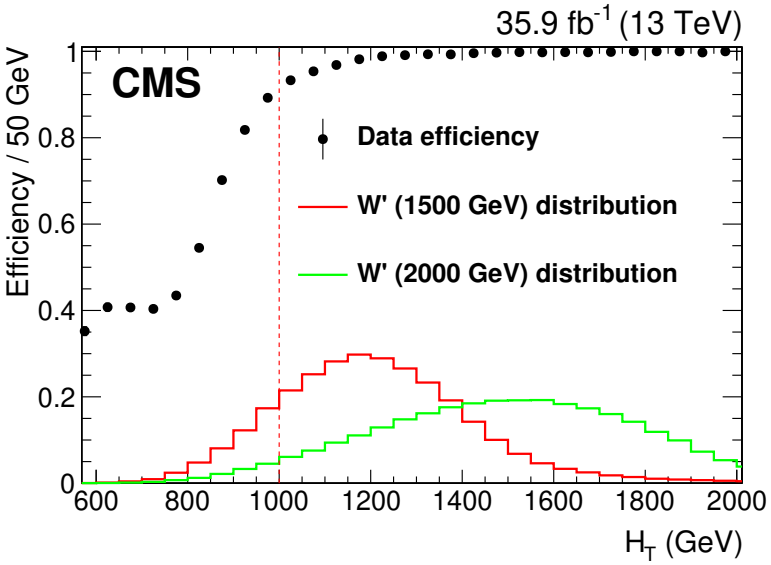

Figure 2. Trigger efficiency as a function of H_T. Events are required to have $H_T > 1\,\text{TeV}$ as is indicated by the red dashed line. The H_T distributions of two W′ signal hypotheses are shown for comparison, normalized to unit area.

Because the signal of interest is a high mass resonance decaying to multiple high-p_T jets, data events are triggered by $H_T > 800$ or $900\,\text{GeV}$, where H_T is defined as the sum of all AK4 jet p_T in the event, or a AK8 jet $p_T > 450\,\text{GeV}$. The signal of interest usually fulfills the high H_T trigger requirement, and the AK8 jet p_T trigger is included to overcome an issue in the trigger H_T calculation that impacts about 24% of the analyzed data.

The efficiency of the trigger selection is studied using a sample of events that have at least one muon of $p_T > 24\,\text{GeV}$. The fraction of these events that pass the full trigger selection is defined as the trigger efficiency and is shown in figure 2 as a function of H_T. The offline event selection requires that H_T be larger than 1 TeV which ensures that the trigger efficiency is larger than 93% near the threshold and is nearly 100% over most of the signal region. Although there is little inefficiency due to the trigger, this is taken into account as an event weight when processing MC samples.

4.1 Top jet tagging

For top quarks with $p_T > 400\,\text{GeV}$, the decay products, one b quark and two light quarks, can merge into a single AK8 jet. Top quark jets are identified using a set of three quantities defined below.

The N-subjettiness [40] algorithm defines the τ_N variable, which quantifies how consistent the jet energy pattern is with N or fewer hard partons, with the low τ_N values being more consistent with N or fewer partons. In the case of a top quark hadronic decay, the ratio of τ_3 to τ_2 is used.

The merged top jet can also be discriminated from background by using the large top quark mass. The modified mass drop tagger algorithm [41], also known as the "soft drop"

JHEP03(2019)127

algorithm [42] with $\beta = 0$ and $z = 0.1$ is used to calculate this mass variable, $m_{\mathrm{SD}}^{\mathrm{t}}$. This algorithm declusters the jet, and removes soft radiations, thus allowing a clearer separation between the merged top jet and background.

Finally, as the top jet contains a b quark, additional discrimination power can be achieved by using subjet b tagging with the combined secondary vertex version 2 (CSVv2) b tagging algorithm (SJ_{csvmax}) [43]. We use a b tagging operating point defined by a 10% misidentification probability with approximately an 80% efficiency.

The MC to data correction (scale factor) for the top tagging operating point in table 1 is measured to be $1.07^{+0.11}_{-0.04}$ in a sample enriched in semileptonic $\mathrm{t\bar{t}}$ production, using the same procedure as outlined in ref. [39].

4.2 Higgs jet tagging

In the case of a highly boosted Higgs boson in the $\mathrm{b\bar{b}}$ decay mode, the decay products tend to merge into a jet that has a mass consistent with a Higgs boson and that contains two b hadrons clustered into the jet. Once again, the soft drop algorithm is used to provide the variable $m_{\mathrm{SD}}^{\mathrm{H}}$ as a measure of the Higgs boson jet mass, but in this case the jet is scaled using a simulation-derived correction suitable for resonances below the top jet tagging mass window [44], which is p_{T} and η dependent but results in a 5-10% mass amplification in both data and MC. Scale factors are used for the jet mass scale and resolution, which are derived from a fit to the distribution of the W boson jet $m_{\mathrm{SD}}^{\mathrm{H}}$ spectrum in a sample enriched in semileptonic $\mathrm{t\bar{t}}$ production using the technique outlined in ref. [39].

To identify the two b quarks clustered into the merged Higgs jet, a dedicated double-b tagging algorithm (Dbtag) is used at an operating point with a misidentification probability of approximately 3% and an efficiency of 50%. Data samples enriched in QCD produced $\mathrm{b\bar{b}}$ and $\mathrm{t\bar{t}}$ events are used to establish scale factors for this tagger for the cases of signal and mistagged top quarks, respectively [43].

Figure 3 shows the variable distributions that are used for top and Higgs candidate jet tagging in $\mathrm{t\bar{t}}$, QCD, and signal MC simulation. The selections for these distributions includes all other top and Higgs candidate jet selections in order to preserve variable correlations.

In the rare occurrence that a jet passes both the Higgs and top jet tags, the ambiguity is resolved by giving the Higgs jet tag priority.

4.3 b jet tagging

The b quark from the VLQ or W' decay is reconstructed as an AK4 jet that is required to pass the CSVv2 b tagging algorithm [43] at the same operating point as is used for the subjets of the merged top jet. A MC to data scale factor for the b tagging requirement is used in order to improve the agreement of data and simulation.

4.4 Event selection

Event selection details can be found in table 1. The signal region used for setting cross section upper limits is required to contain a top, a Higgs boson, and a b tagged jet.

JHEP03(2019)127

Label	Discriminator selections
H_{tag}	Dbtag > 0.8 and $105 < m^{H}_{SD} < 135\,GeV$
t_{tag}	$SJ_{csvmax} > 0.5426$ and $\tau_3/\tau_2 < 0.8$ and $105 < m^{t}_{SD} < 210\,GeV$
b_{tag}	CSVv2 > 0.5426
$H_{antitag}$	$m^{H}_{SD} < 30\,GeV$
$t_{antitag}$	$SJ_{csvmax} > 0.5426$ and $\tau_3/\tau_2 > 0.65$ and $30 < m^{t}_{SD} < 105\,GeV$
$b_{antitag}$	CSVv2 < 0.5426

Signal region			
Region	Top jet	Higgs jet	b jet
SR	t_{tag}	H_{tag}	b_{tag}

Validation region			
Region	Top jet	Higgs jet	b jet
VR	t_{tag}	H_{tag}	$b_{antitag}$

Background estimation			
Region	Top jet	Higgs jet	b jet
CR1	$t_{antitag}$	$H_{antitag}$	b_{tag}
CR2	$t_{antitag}$	H_{tag}	b_{tag}
CR3	t_{tag}	$H_{antitag}$	b_{tag}

Validation background estimation			
Region	Top jet	Higgs jet	b jet
CR4	$t_{antitag}$	$H_{antitag}$	$b_{antitag}$
CR5	$t_{antitag}$	H_{tag}	$b_{antitag}$
CR6	t_{tag}	$H_{antitag}$	$b_{antitag}$

Table 1. Selection regions used in the analysis. Tagging discriminator selections and regions described in the text are explicitly defined here. The signal region (SR) is used to set cross section upper limits, the control regions (CRN) are used to estimate the QCD background, and the validation region (VR) is used to validate the background estimation procedure.

	$m_{W'}$(GeV)					
m_{VLQ}(GeV)	1500	2000	2500	3000	3500	4000
800	0.70 ± 0.13					
1000	0.91 ± 0.18	2.3 ± 0.4				
1300	0.48 ± 0.09	2.6 ± 0.4	3.7 ± 0.6			
1500		2.1 ± 0.4	3.7 ± 0.6	4.2 ± 0.7		
1800			3.2 ± 0.5	4.1 ± 0.7	4.4 ± 0.7	
2100				3.7 ± 0.6	4.2 ± 0.7	4.4 ± 0.7
2500					3.8 ± 0.6	4.0 ± 0.7
3000						3.4 ± 0.6

Table 2. The selection efficiency (%) for each signal mass point in the analysis.

The sensitivity of the selections used in the analysis have been studied both in the context of the expected limit and the W′ discovery potential. After identifying the top, Higgs, and b candidate jets, the W′ candidate mass is analyzed as the invariant mass of the three jets. Table 2 shows the signal efficiency for all samples considered in the analysis.

JHEP03(2019)127

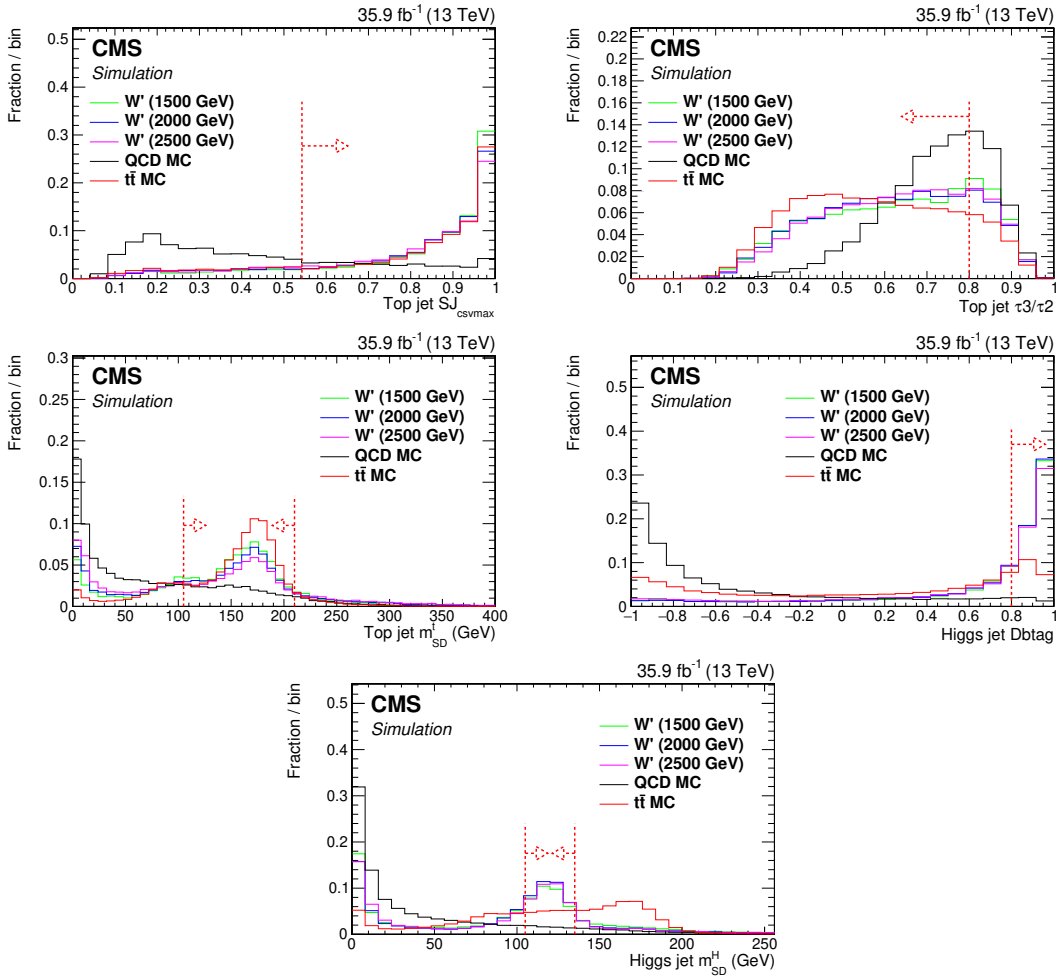

Figure 3. Normalized distributions of the discriminating variables in $t\bar{t}$, QCD, and signal MC simulation. The distributions shown, from upper left to lower right, are of the variables: the maximum subjet b tag, τ_3/τ_2, and m^{t}_{SD}, all used for top quark discrimination, and the double-b tag discriminant and m^{H}_{SD} used for tagging candidate Higgs boson jets. The QCD distributions are extracted from events with the generator-level $H_T > 1$ TeV. Each variable distribution in this set of figures requires an event that passes the selection on all other variables in order to preserve possible correlations.

5 Background estimation

The primary background in this analysis is QCD multijet production, the contribution of which is derived from data using control regions that are selected with kinematic criteria that are similar to those used for the signal region but with a reduced signal efficiency. This is achieved by inverting top substructure selections and extracting the Higgs jet pass to fail ratio for QCD jets. This ratio is then used as an event weight for events that pass the top jet selection but fail the Higgs boson jet selection. The resulting distribution is used as the background estimate for the signal region. The primary assumption for the background estimate method is that the top jet substructure selection can be inverted without largely biasing the Higgs jet substructure selection.

JHEP03(2019)127

A set of control regions are defined by requiring the Higgs jet candidate $m_{\mathrm{SD}}^{\mathrm{H}}$ to be less than 30 GeV with no double-b tagging selection. Table 1 defines various selection regions used in the analysis. A transfer function $F(p_{\mathrm{T}}, \eta)$ is extracted from data by inverting the top jet candidate $m_{\mathrm{SD}}^{\mathrm{t}}$ selection to be between 30 and 105 GeV and $\tau_3/\tau_2 > 0.65$. In this region, $F(p_{\mathrm{T}}, \eta)$ is defined as the ratio of the jet p_{T} spectrum of the tagged Higgs candidate in two η regions (central, $|\eta| < 1.0$, and forward, $|\eta| > 1.0$) for the full Higgs jet selection (CR2) to the inverted selection (CR1) and is shown in figure 4. The $F(p_{\mathrm{T}}, \eta)$ distribution is used to transform the normalization and shape of distributions from the $\mathrm{H}_{\mathrm{antitag}}$ region to the $\mathrm{H}_{\mathrm{tag}}$ selection region, and is measured with low signal contamination.

The $F(p_{\mathrm{T}}, \eta)$ function is then used to predict the background in the signal region. This is accomplished by defining a control region in data with identical top and b jet candidate selections as in the signal region, but with the inverted Higgs jet selection (CR3). In this region, the m_{tHb} template is created using $F(p_{\mathrm{T}}, \eta)$ as an event weight in a given Higgs candidate jet p_{T}, η bin. This weighted template is used as the QCD background estimate in the signal region.

In the $F(p_{\mathrm{T}}, \eta)$ extraction procedure, the $\mathrm{t\bar{t}}$ production component is subtracted from data in all distributions used for creating $F(p_{\mathrm{T}}, \eta)$ in order to ensure that $F(p_{\mathrm{T}}, \eta)$ refers only to the QCD component. The fraction of $\mathrm{t\bar{t}}$ simulation subtracted from the numerator and denominator is low, 7.3 and 0.4% of the total distribution, respectively. Additionally, the $\mathrm{t\bar{t}}$ contamination of the QCD background estimate in the signal region must to be subtracted. This is performed by applying the QCD background estimation procedure to simulated $\mathrm{t\bar{t}}$ events using the same $F(p_{\mathrm{T}}, \eta)$ as is used when extracting the QCD estimate from data. The estimated contribution accounts for 2.6% of the total QCD estimate in the signal region, which is then subtracted when forming the background estimate. The $\mathrm{t\bar{t}}$ contamination has only a small effect on the QCD background estimation, so the systematic uncertainty due to the $\mathrm{t\bar{t}}$ subtraction procedure is conservatively taken as the difference between the QCD background estimate extracted with and without the full $\mathrm{t\bar{t}}$ subtraction procedure.

In order to test the applicability and versatility of the background estimate in data, a validation region, VR as defined in table 1, is defined based on inverting the b tagging criterion on the b candidate jet, with the corresponding control regions for background estimation (CR4–CR6). The transfer function in this validation region $F_{\mathrm{v}}(p_{\mathrm{T}}, \eta)$ is estimated from the ratio of CR5 to CR4 using the same parameterization as $F(p_{\mathrm{T}}, \eta)$. The m_{tHb} background validation test in this region can be seen in figure 5. This region validates the background estimate analog with a χ^2/ndf of 0.3 with systematic uncertainties taken into account, where ndf is the number of degrees of freedom. The $\mathrm{t\bar{t}}$ component in this validation region is removed using the same procedure that is used in the signal region background estimate. The agreement in the m_{tHb} distribution background validation test demonstrates that the top jet selection can be inverted without biasing the Higgs jet selection. The Higgs jet candidate 4-vector mass for the SR background estimate is set to the mean of the distribution extracted from the VR in order to correct the small kinematic bias from the mass selection when forming the m_{tHb} invariant mass. This correction has only a small effect on the resulting distribution because of the fact that the jet p_{T} is large

JHEP03(2019)127

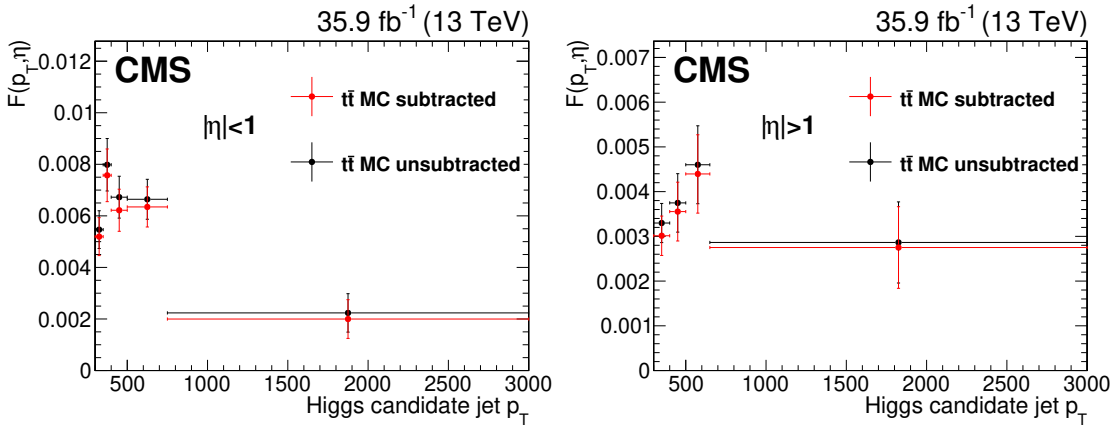

Figure 4. Transfer function $F(p_{\mathrm{T}}, \eta)$ used for estimation of the QCD background in the signal region, shown in the central (left) and forward (right) η regions. The error bars represent the statistical uncertainty in $F(p_{\mathrm{T}}, \eta)$ only.

compared to the mass, and a systematic uncertainty is evaluated as the root mean square of the distribution in the VR.

Additionally, the background validation can be studied with simulated QCD events. Figure 6 shows the level of background agreement where the SR selection and QCD background are evaluated using only simulated QCD events with the same method as was previously described for data. A χ^2/ndf of 1.4 is observed, and an additional systematic uncertainty is included when evaluating the QCD background estimate in collision data. This correction is extracted from the ratio of the SR to QCD background in the QCD MC validation test, and is applied using an interpolation of the ratio in order to decrease the effect of statistical fluctuations but to still keep the increased uncertainty at low m_{tHb}.

The $\mathrm{t\bar{t}}$ component is estimated by using simulation with an additional event weight to correct the generator top jet p_{T} distribution [45]. This generator correction is used in order to improve the agreement of MC with data with respect to a known generator level mismodelling and is cross checked in the VR region.

6 Systematic uncertainties

This analysis considers a wide range of systematic uncertainties that are organized into those that impact only the event yields, which are assumed to follow a log-normal distribution [46], and those that affect the m_{tHb} distribution shape as well. All of the systematic uncertainties considered in the analysis are summarized in table 3.

6.1 Normalization uncertainties

The uncertainty in the integrated luminosity is taken as 2.5% for the data set used in the analysis [21].

The uncertainty in the correction to the efficiency of top jet tagging algorithm is between −4 and +10% of the nominal value.

JHEP03(2019)127

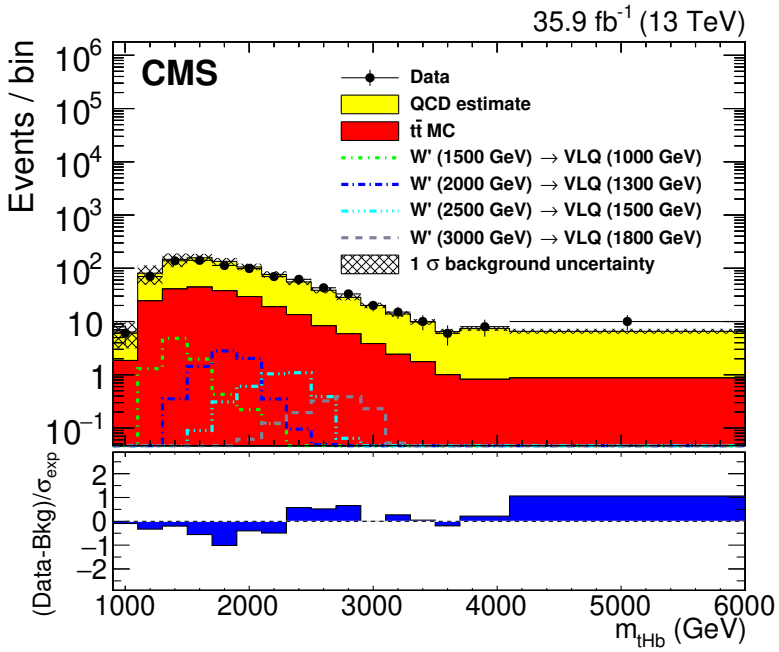

Figure 5. Reconstructed W′ mass distributions (m_{tHb}) in the b candidate inverted validation region (VR) shown for data and background contributions. Several signal hypotheses are shown to demonstrate the low signal contamination. The background uncertainty includes all systematic and statistical uncertainties.

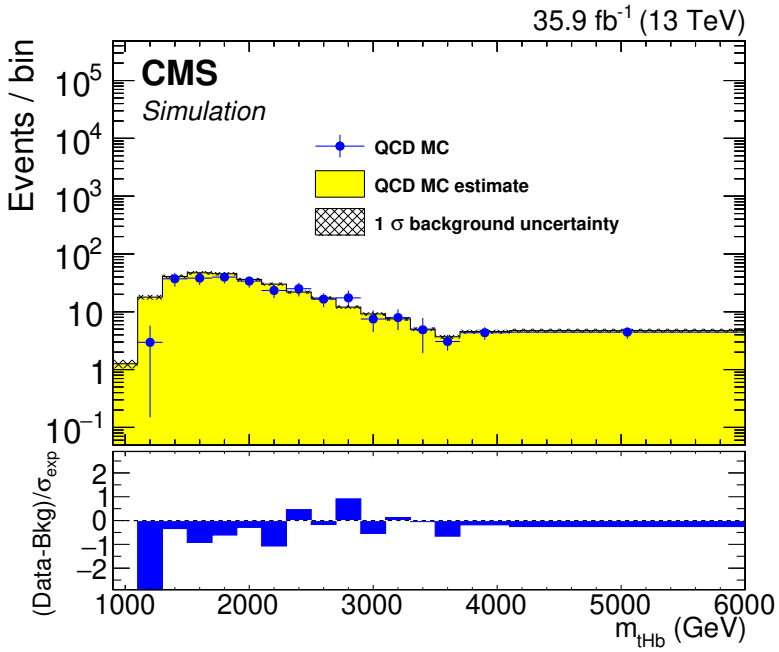

Figure 6. Reconstructed W′ mass distributions (m_{tHb}) for the simulated QCD events in the signal region for the purposes of validation. The agreement given the systematic uncertainties is at the 1 standard deviation level. The background uncertainty takes into account all systematic and statistical uncertainties.

JHEP03(2019)127

The theoretical uncertainty in the $t\bar{t}$ production cross section is taken into account as an asymmetric uncertainty between -5.5 and $+4.8\%$ that is calculated as the quadrature sum of the scale and PDF uncertainties on the overall cross section.

6.2 Shape uncertainties

The uncertainty in the jet energy scale is taken into account by scaling the four-vectors used in reconstructing the m_{tHb} distribution by the $\pm 1\sigma$ jet energy scale uncertainty, which is approximately 2% for jets in the analysis. The jet energy scale variation impacts the m_{tHb} distribution shape through a horizontal shift but can also cause a normalization difference in the case that the jet falls above or below the kinematic threshold. The uncertainty in the jet energy resolution is also taken into account by the $\pm 1\sigma$ uncertainty in the jet energy resolution correction used for simulated samples. This uncertainty is applied to all simulated samples used in the analysis, and has only a small impact.

The uncertainty in the jet mass scale and resolution is measured in a highly enriched sample of $t\bar{t}$ containing one final state lepton. In this sample, a fit is performed to the W boson jet mass peak in the corresponding AK8 jet PUPPI $m_{\mathrm{SD}}^{\mathrm{H}}$ distribution, in which the mean and width of the PUPPI $m_{\mathrm{SD}}^{\mathrm{H}}$ spectrum is extracted. The mass scale uncertainty is estimated from the shift of the W mass peak to be 0.94%. The uncertainty in the mass resolution is estimated from the W boson mass peak width to be 20%. These uncertainties are applied to the signal estimate used in the analysis, and result in approximately 4 and 6% variations in the overall yield for the scale and resolution uncertainties, respectively. The differences in the W and Higgs boson tagging efficiencies are estimated from a comparison of parton showering methods and are found to be between 4–5%, so an additional 5% uncertainty is included for the signal simulated samples used in the analysis.

The uncertainty used for the b tagging requirement on the AK4 jet is evaluated by varying the b tagging and b mistagging scale factor within their $\pm 1\sigma$ uncertainty and are considered uncorrelated with each other. Given the kinematic selection on the AK4 jet, this uncertainty is evaluated in four p_{T} regions from 200–1000 GeV. For jets with a p_{T} outside of this region, the uncertainty is evaluated as twice the uncertainty at 1000 GeV. This uncertainty is applied to all simulated samples used in the analysis, and results in approximately a 2% effect.

The double-b tagging uncertainty used for the Higgs jet tagging [43] selection is evaluated by varying the double-b tagging scale factor by the $\pm 1\sigma$ uncertainty. The scale factor is parameterized using three regions in p_{T}. Similar to the AK4 b tagging uncertainty, outside of the kinematic range of the scale factor, the uncertainty is evaluated at twice the maximum range. The double-b tagging scale factor uncertainty results in approximately a 5% effect. Also evaluated is the mistag scale factor in the case of a Higgs boson mistagged as a top quark, as explained in section 4. The uncertainties in both the Higgs jet tagging efficiency and the mistag rate are applied to all simulated samples used in the analysis, and are treated as uncorrelated with each other during limit setting.

The events used by the analysis are largely collected where the trigger efficiency is near 100%, however the small inefficiency is evaluated using the trigger efficiency extracted from data as parameterized in H_{T} (see figure 2), and the uncertainty is evaluated as half of

JHEP03(2019)127

this inefficiency. This uncertainty is small (<1%), and is applied to all simulated samples used in the analysis.

As mentioned in section 3, the simulated pileup distribution is reweighted to match data using an effective total inelastic cross section of 69.2 mb. The uncertainty in this procedure is evaluated by varying the total inelastic cross section by ±4.6% [47]. This uncertainty is applied to all simulated samples used in the analysis, and has only a small impact.

The m_{tHb} distribution from the $\mathrm{t\bar{t}}$ simulation is reweighted to correct for known differences in the generator p_{T} spectrum [45]. The $\pm1\sigma$ shape uncertainty in this procedure is estimated from the difference with the unweighted distribution. This uncertainty is applied to the $\mathrm{t\bar{t}}$ simulated sample used in the analysis, and results in approximately a 21% effect.

The PDF uncertainty is evaluated using the NNPDF3.0 set [48]. The NNPDF set uses MC replicas, from which the uncertainty is evaluated as the RMS of the distribution of the associated weights, and is then added in quadrature with the α_s uncertainty. In the case of signal, the shapes are then normalized to the nominal distribution, as to only preserve the shape of the PDF uncertainty. The normalization component of the PDF uncertainty is considered an uncertainty in the signal cross section.

The renormalization and factorization (μ_{R} and μ_{F}) scale uncertainty is evaluated using event weights provided for varying the μ_{R} or μ_{F} scales up and down by a factor of two. There are six total weights that represent the independent and simultaneous variation of μ_{R} and μ_{F}. Per event, all weights are considered and the envelope is then used as the $\pm1\sigma$ uncertainty band. This uncertainty is applied to the $\mathrm{t\bar{t}}$ MC sample used in the analysis, and results in an approximately 30% effect. Similar to the PDF uncertainty, the normalization component of this uncertainty is taken as the signal cross section theoretical uncertainty, and the shape component alone is used for limit setting.

The analysis considers five sources of uncertainty in the shape of the QCD background estimate derived from data. The statistical uncertainty in $F(p_{\mathrm{T}}, \eta)$ is propagated to the m_{tHb} spectrum by evaluating the $F(p_{\mathrm{T}}, \eta)$ weight at $\pm1\sigma$ in a given (p_{T}, η) bin. The uncertainty from each $F(p_{\mathrm{T}}, \eta)$ bin is added in quadrature to form the full uncertainty in the m_{tHb} template. The up and down uncertainty variation in the $\mathrm{t\bar{t}}$ subtraction procedure is taken as the unsubtracted m_{tHb} distribution and the resulting m_{tHb} distribution given twice the subtraction. The uncertainty in the four vector Higgs jet candidate mass modification is taken as ±30 GeV. The "nonclosure" uncertainty in the QCD background estimate is evaluated as the difference between the full selection and background prediction from the QCD MC closure test using the interpolated ratio, and is the leading source of uncertainty in the QCD background estimate of approximately 20%.

The MC statistical uncertainty is taken into account using the "Barlow-Beeston lite" method [49] during limit setting.

7 Results

The final m_{tHb} distribution is shown in figure 7, with a χ^2/ndf of 1.3 for the agreement of data and background. Table 4 shows the yield for data, QCD and $\mathrm{t\bar{t}}$ backgrounds, for various selection regions including the full selection.

JHEP03(2019)127

Source	Variation	Process
Integrated luminosity	$\pm 2.5\%$	signal, $\mathrm{t\bar{t}}$
Top jet tagging	$+10.0\%$, -4%	signal, $\mathrm{t\bar{t}}$
$\mathrm{t\bar{t}}$ cross section	$+4.8\%$, -5.5%	$\mathrm{t\bar{t}}$
Top quark p_{T} reweighting	$+1\sigma(p_{\mathrm{T}}(\mathrm{gen}))$	$\mathrm{t\bar{t}}$
Matrix element $\mu_{\mathrm{R}}/\mu_{\mathrm{F}}$ scales	$\pm 1\sigma(\mu_{\mathrm{R}}/\mu_{\mathrm{F}})$	signal, $\mathrm{t\bar{t}}$
Jet energy scale	$\pm 1\sigma(p_{\mathrm{T}}, \eta)$	signal, $\mathrm{t\bar{t}}$
Jet energy resolution	$\pm 1\sigma(p_{\mathrm{T}}, \eta)$	signal, $\mathrm{t\bar{t}}$
Jet mass scale	$\pm 1\sigma(m^{\mathrm{H}}_{\mathrm{SD}})$	signal, $\mathrm{t\bar{t}}$
Jet mass resolution	$\pm 1\sigma(m^{\mathrm{H}}_{\mathrm{SD}})$	signal, $\mathrm{t\bar{t}}$
b tagging	$\pm 1\sigma(p_{\mathrm{T}})$	signal, $\mathrm{t\bar{t}}$
b mistagging	$\pm 1\sigma(p_{\mathrm{T}})$	signal, $\mathrm{t\bar{t}}$
Double-b tagging	$\pm 1\sigma(p_{\mathrm{T}})$	signal, $\mathrm{t\bar{t}}$
Double-b mistagging	$\pm 1\sigma(p_{\mathrm{T}})$	signal, $\mathrm{t\bar{t}}$
Higgs jet tagging	$\pm 5\%$	signal
Pileup	$\pm 1\sigma$ (σ_{mb})	signal, $\mathrm{t\bar{t}}$
PDF	$\pm 1\sigma(Q^2, x)$	signal, $\mathrm{t\bar{t}}$
H_{T} trigger	$\pm 1\sigma(H_{\mathrm{T}})$	signal, $\mathrm{t\bar{t}}$
$\mathrm{t\bar{t}}$ contamination	$\pm 1\sigma(p_{\mathrm{T}})$	QCD
$F(p_{\mathrm{T}}, \eta)$	$\pm 1\sigma(p_{\mathrm{T}}, \eta)$	QCD
Higgs jet mass modification	$\pm 1\sigma(m_{\mathrm{H}})$	QCD
Nonclosure	$\pm 1\sigma(m_{\mathrm{tHb}})$	QCD

Table 3. Sources of systematic uncertainty affecting the m_{tHb} distribution. Sources that list the systematic variation as $\pm 1\sigma$ depend on the distribution of the variable given in the parentheses, while those that list the variation in percent are rate uncertainties.

Region	Data	QCD	$\mathrm{t\bar{t}}$
CR1	79 104	—	332
CR2	398	—	25
CR3	45 646	—	1365
CR4	288 926	—	543
CR5	1 330	—	76
CR6	154 608	—	1991
VR	844 ± 30	659 ± 150	236 ± 83
SR	284 ± 17	208 ± 49	71 ± 28

Table 4. Event yield table after various selections. The definition of each region is given in table 1. The uncertainties shown here for the validation region and the signal region are pre fit; the posteriori uncertainties for $\mathrm{t\bar{t}}$ and QCD are constrained down by 40 and 14%, respectively.

JHEP03(2019)127

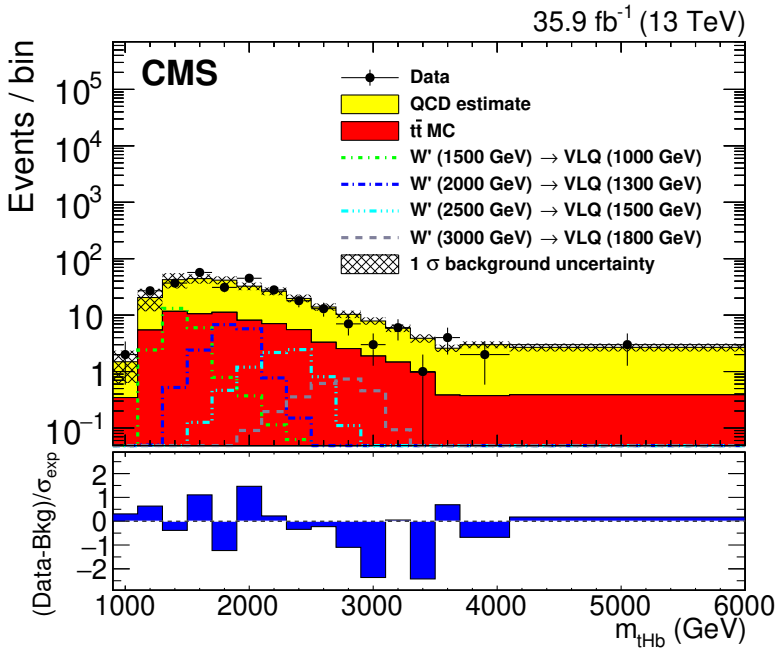

Figure 7. Reconstructed W′ mass distributions (m_{tHb}) in the signal region, compared with the distributions of estimated backgrounds, and several benchmarks models. The signal distributions include the contributions from W′ decays to both the T and B assuming equal branching fractions. The uncertainties shown in the hatched region contain both statistical and systematic uncertainties of all background components.

Using a Bayesian approach with a flat prior for the signal cross section, upper limits are obtained on the product of the W′ boson production cross section in the $s_{\mathrm{L}} = 0.5$ and $\cot(\theta_2) = 3$ hypothesis, and the benchmark $\mathrm{W}' \to \mathrm{T/B} \to \mathrm{tHb}$ branching fraction. A binned likelihood is used to calculate 95% confidence level (CL) upper limits, in a process where all systematic uncertainties listed in section 6 that affect the shape of the m_{tHb} distribution are included as nuisance parameters that modify the shape using template interpolation, and those that affect the normalization are included as nuisance parameters with lognormal priors. For the signal template, the sum of reconstructed m_{tHb} distribution from the tB and bT decay channels is used.

Pseudo-experiments are used to derive the $\pm 1\sigma$ deviations in the expected limit. The systematic uncertainties described above are accounted for as nuisance parameters and the posterior probability is refitted for each pseudo-experiment. Cross section upper limits are shown in figure 8. The highest signal significance is at $M_{\mathrm{W}'} = 2\,\mathrm{TeV}$ from the high VLQ mass hypothesis at a value of 0.85 standard deviations. Although no signal mass points are excluded by solely analyzing the all hadronic $\mathrm{W}' \to \mathrm{T/B} \to \mathrm{tHb}$ decay in the democratic bT and tB decay hypothesis, a W′ with a mass below 1.6 TeV is excluded at 95% CL in the case of a 100% bT branching fraction hypothesis.

JHEP03(2019)127

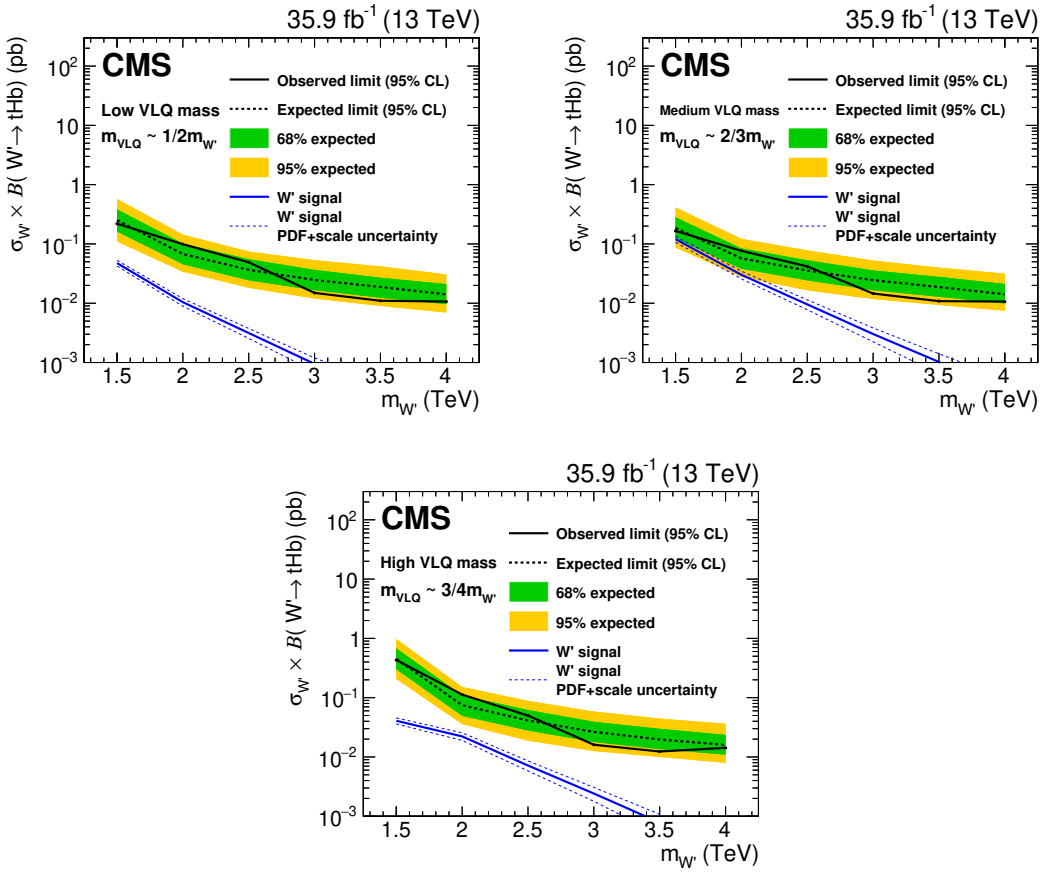

Figure 8. The W′ boson 95% CL production cross section limits. The expected limits (dashed) and observed limits (solid), as well as the W′ boson theoretical cross section and the PDF and scale normalization uncertainties are shown. The bands around the expected limit represent the ±1 and $\pm 2\sigma_{exp}$ uncertainties in the expected limit. The limits for low- (upper left), medium- (upper right), and high- (lower) mass VLQ mass ranges, defined in table 2, are shown.

8 Summary

A search for a heavy W′ boson decaying to a B or T vector-like quark and a top or b quark, respectively, has been presented. The data correspond to an integrated luminosity of 35.9 fb^{-1} collected in 2016 with the CMS detector at the LHC. The signature considered for both decay modes is a top quark and a Higgs boson, both decaying hadronically, and a b quark jet. Boosted heavy-resonance identification techniques are used to exploit the event signature of three energetic jets and to suppress standard model backgrounds. No significant deviation from the standard model background prediction has been observed. Cross section upper limits on W′ boson production in the top quark, Higgs boson, and b quark decay mode are set as a function of the W′ mass, for several vector-like quark mass hypotheses. These are the first limits for W′ boson production in this decay channel, and cover a range of 0.01 to 0.43 pb in the W′ mass range between 1.5 and 4.0 TeV.

JHEP03(2019)127

Acknowledgments

We congratulate our colleagues in the CERN accelerator departments for the excellent performance of the LHC and thank the technical and administrative staffs at CERN and at other CMS institutes for their contributions to the success of the CMS effort. In addition, we gratefully acknowledge the computing centers and personnel of the Worldwide LHC Computing Grid for delivering so effectively the computing infrastructure essential to our analyses. Finally, we acknowledge the enduring support for the construction and operation of the LHC and the CMS detector provided by the following funding agencies: BMBWF and FWF (Austria); FNRS and FWO (Belgium); CNPq, CAPES, FAPERJ, FAPERGS, and FAPESP (Brazil); MES (Bulgaria); CERN; CAS, MoST, and NSFC (China); COLCIENCIAS (Colombia); MSES and CSF (Croatia); RPF (Cyprus); SENESCYT (Ecuador); MoER, ERC IUT, and ERDF (Estonia); Academy of Finland, MEC, and HIP (Finland); CEA and CNRS/IN2P3 (France); BMBF, DFG, and HGF (Germany); GSRT (Greece); NKFIA (Hungary); DAE and DST (India); IPM (Iran); SFI (Ireland); INFN (Italy); MSIP and NRF (Republic of Korea); MES (Latvia); LAS (Lithuania); MOE and UM (Malaysia); BUAP, CINVESTAV, CONACYT, LNS, SEP, and UASLP-FAI (Mexico); MOS (Montenegro); MBIE (New Zealand); PAEC (Pakistan); MSHE and NSC (Poland); FCT (Portugal); JINR (Dubna); MON, RosAtom, RAS, RFBR, and NRC KI (Russia); MESTD (Serbia); SEIDI, CPAN, PCTI, and FEDER (Spain); MOSTR (Sri Lanka); Swiss Funding Agencies (Switzerland); MST (Taipei); ThEPCenter, IPST, STAR, and NSTDA (Thailand); TUBITAK and TAEK (Turkey); NASU and SFFR (Ukraine); STFC (United Kingdom); DOE and NSF (U.S.A.).

Individuals have received support from the Marie-Curie program and the European Research Council and Horizon 2020 Grant, contract No. 675440 (European Union); the Leventis Foundation; the A. P. Sloan Foundation; the Alexander von Humboldt Foundation; the Belgian Federal Science Policy Office; the Fonds pour la Formation à la Recherche dans l'Industrie et dans l'Agriculture (FRIA-Belgium); the Agentschap voor Innovatie door Wetenschap en Technologie (IWT-Belgium); the F.R.S.-FNRS and FWO (Belgium) under the "Excellence of Science - EOS" - be.h project n. 30820817; the Ministry of Education, Youth and Sports (MEYS) of the Czech Republic; the Lendület ("Momentum") Programme and the János Bolyai Research Scholarship of the Hungarian Academy of Sciences, the New National Excellence Program ÚNKP, the NKFIA research grants 123842, 123959, 124845, 124850 and 125105 (Hungary); the Council of Science and Industrial Research, India; the HOMING PLUS program of the Foundation for Polish Science, cofinanced from European Union, Regional Development Fund, the Mobility Plus program of the Ministry of Science and Higher Education, the National Science Center (Poland), contracts Harmonia 2014/14/M/ST2/00428, Opus 2014/13/B/ST2/02543, 2014/15/B/ST2/03998, and 2015/19/B/ST2/02861, Sonata-bis 2012/07/E/ST2/01406; the National Priorities Research Program by Qatar National Research Fund; the Programa Estatal de Fomento de la Investigación Científica y Técnica de Excelencia María de Maeztu, grant MDM-2015-0509 and the Programa Severo Ochoa del Principado de Asturias; the Thalis and Aristeia program cofinanced by EU-ESF and the Greek NSRF; the Rachadapisek Sompot Fund for

JHEP03(2019)127

Postdoctoral Fellowship, Chulalongkorn University and the Chulalongkorn Academic into Its 2nd Century Project Advancement Project (Thailand); the Welch Foundation, contract C-1845; and the Weston Havens Foundation (U.S.A.).

References

[1] M. Schmaltz and D. Tucker-Smith, *Little Higgs theories*, *Ann. Rev. Nucl. Part. Sci.* **55** (2005) 229 [hep-ph/0502182] [INSPIRE].

[2] T. Appelquist, H.-C. Cheng and B.A. Dobrescu, *Bounds on universal extra dimensions*, *Phys. Rev.* **D 64** (2001) 035002 [hep-ph/0012100] [INSPIRE].

[3] R.N. Mohapatra and J.C. Pati, *Left-right gauge symmetry and an 'isoconjugate' model of CP violation*, *Phys. Rev.* **D 11** (1975) 566 [INSPIRE].

[4] CMS collaboration, *Search for heavy gauge W' boson in events with an energetic lepton and large missing transverse momentum at* $\sqrt{s} = 13$ *TeV*, *Phys. Lett.* **B 770** (2017) 278 [arXiv:1612.09274] [INSPIRE].

[5] ATLAS collaboration, *Search for a new heavy gauge boson resonance decaying into a lepton and missing transverse momentum in 36* fb^{-1} *of pp collisions at* $\sqrt{s} = 13$ *TeV with the ATLAS experiment*, *Eur. Phys. J.* **C 78** (2018) 401 [arXiv:1706.04786] [INSPIRE].

[6] CMS collaboration, *Search for a heavy resonance decaying to a pair of vector bosons in the lepton plus merged jet final state at* $\sqrt{s} = 13$ *TeV*, *JHEP* **05** (2018) 088 [arXiv:1802.09407] [INSPIRE].

[7] ATLAS collaboration, *Search for WW/WZ resonance production in* $\ell\nu qq$ *final states in pp collisions at* $\sqrt{s} = 13$ *TeV with the ATLAS detector*, *JHEP* **03** (2018) 042 [arXiv:1710.07235] [INSPIRE].

[8] CMS collaboration, *Searches for W' bosons decaying to a top quark and a bottom quark in proton-proton collisions at 13 TeV*, *JHEP* **08** (2017) 029 [arXiv:1706.04260] [INSPIRE].

[9] ATLAS collaboration, *Search for* $W' \to tb$ *decays in the hadronic final state using pp collisions at* $\sqrt{s} = 13$ *TeV with the ATLAS detector*, *Phys. Lett.* **B 781** (2018) 327 [arXiv:1801.07893] [INSPIRE].

[10] CMS collaboration, *Search for single production of a vector-like T quark decaying to a Z boson and a top quark in proton-proton collisions at* $\sqrt{s} = 13$ *TeV*, *Phys. Lett.* **B 781** (2018) 574 [arXiv:1708.01062] [INSPIRE].

[11] CMS collaboration, *Search for single production of vector-like quarks decaying to a b quark and a Higgs boson*, *JHEP* **06** (2018) 031 [arXiv:1802.01486] [INSPIRE].

[12] ATLAS collaboration, *Search for pair- and single-production of vector-like quarks in final states with at least one Z boson decaying into a pair of electrons or muons in pp collision data collected with the ATLAS detector at* $\sqrt{s} = 13$ *TeV*, *Phys. Rev.* **D 98** (2018) 112010 [arXiv:1806.10555] [INSPIRE].

[13] CMS collaboration, *Search for single production of vector-like quarks decaying into a b quark and a W boson in proton-proton collisions at* $\sqrt{s} = 13$ *TeV*, *Phys. Lett.* **B 772** (2017) 634 [arXiv:1701.08328] [INSPIRE].

JHEP03(2019)127

[14] CMS collaboration, *Search for pair production of vector-like quarks in the $bW\bar{b}W$ channel from proton-proton collisions at $\sqrt{s} = 13$ TeV*, *Phys. Lett.* **B 779** (2018) 82 [arXiv:1710.01539] [INSPIRE].

[15] CMS collaboration, *Search for vector-like T and B quark pairs in final states with leptons at $\sqrt{s} = 13$ TeV*, *JHEP* **08** (2018) 177 [arXiv:1805.04758] [INSPIRE].

[16] ATLAS collaboration, *Combination of the searches for pair-produced vector-like partners of the third-generation quarks at $\sqrt{s} = 13$ TeV with the ATLAS detector*, *Phys. Rev. Lett.* **121** (2018) 211801 [arXiv:1808.02343] [INSPIRE].

[17] K. Agashe, R. Contino and A. Pomarol, *The minimal composite Higgs model*, *Nucl. Phys.* **B 719** (2005) 165 [hep-ph/0412089] [INSPIRE].

[18] D. Barducci, A. Belyaev, S. De Curtis, S. Moretti and G.M. Pruna, *Exploring Drell-Yan signals from the 4D Composite Higgs Model at the LHC*, *JHEP* **04** (2013) 152 [arXiv:1210.2927] [INSPIRE].

[19] D. Barducci and C. Delaunay, *Bounding wide composite vector resonances at the LHC*, *JHEP* **02** (2016) 055 [arXiv:1511.01101] [INSPIRE].

[20] N. Vignaroli, *New W' signals at the LHC*, *Phys. Rev.* **D 89** (2014) 095027 [arXiv:1404.5558] [INSPIRE].

[21] CMS collaboration, *CMS luminosity measurements for the 2016 data taking period*, CMS-PAS-LUM-17-001 (2017).

[22] CMS collaboration, *The CMS experiment at the CERN LHC*, 2008 *JINST* **3** S08004 [INSPIRE].

[23] CMS collaboration, *Particle-flow reconstruction and global event description with the CMS detector*, 2017 *JINST* **12** P10003 [arXiv:1706.04965] [INSPIRE].

[24] M. Cacciari, G.P. Salam and G. Soyez, *The anti-k_t jet clustering algorithm*, *JHEP* **04** (2008) 063 [arXiv:0802.1189] [INSPIRE].

[25] M. Cacciari, G.P. Salam and G. Soyez, *FastJet user manual*, *Eur. Phys. J.* **C 72** (2012) 1896 [arXiv:1111.6097] [INSPIRE].

[26] D. Bertolini, P. Harris, M. Low and N. Tran, *Pileup per particle identification*, *JHEP* **10** (2014) 059 [arXiv:1407.6013] [INSPIRE].

[27] CMS collaboration, *Jet energy scale and resolution in the CMS experiment in pp collisions at 8 TeV*, 2017 *JINST* **12** P02014 [arXiv:1607.03663] [INSPIRE].

[28] CMS collaboration, *The CMS trigger system*, 2017 *JINST* **12** P01020 [arXiv:1609.02366] [INSPIRE].

[29] S. Frixione, P. Nason and C. Oleari, *Matching NLO QCD computations with Parton Shower simulations: the POWHEG method*, *JHEP* **11** (2007) 070 [arXiv:0709.2092] [INSPIRE].

[30] S. Alioli, P. Nason, C. Oleari and E. Re, *A general framework for implementing NLO calculations in shower Monte Carlo programs: the POWHEG BOX*, *JHEP* **06** (2010) 043 [arXiv:1002.2581] [INSPIRE].

[31] P. Nason, *A new method for combining NLO QCD with shower Monte Carlo algorithms*, *JHEP* **11** (2004) 040 [hep-ph/0409146] [INSPIRE].

[32] S. Frixione, P. Nason and G. Ridolfi, *A positive-weight next-to-leading-order Monte Carlo for heavy flavour hadroproduction*, *JHEP* **09** (2007) 126 [arXiv:0707.3088] [INSPIRE].

JHEP03(2019)127

[33] J. Alwall et al., *The automated computation of tree-level and next-to-leading order differential cross sections and their matching to parton shower simulations*, *JHEP* **07** (2014) 079 [arXiv:1405.0301] [INSPIRE].

[34] J. Alwall et al., *Comparative study of various algorithms for the merging of parton showers and matrix elements in hadronic collisions*, *Eur. Phys. J.* **C 53** (2008) 473 [arXiv:0706.2569] [INSPIRE].

[35] T. Sjöstrand et al., *An introduction to PYTHIA 8.2*, *Comput. Phys. Commun.* **191** (2015) 159 [arXiv:1410.3012] [INSPIRE].

[36] CMS collaboration, *Investigations of the impact of the parton shower tuning in PYTHIA 8 in the modelling of $t\bar{t}$ at $\sqrt{s} = 8$ and 13 TeV*, CMS-PAS-TOP-16-021 (2016).

[37] CMS collaboration, *Event generator tunes obtained from underlying event and multiparton scattering measurements*, *Eur. Phys. J.* **C 76** (2016) 155 [arXiv:1512.00815] [INSPIRE].

[38] GEANT4 collaboration, GEANT4 — *a simulation toolkit*, *Nucl. Instrum. Meth.* **506** (2003) 250.

[39] CMS collaboration, *Jet algorithms performance in 13 TeV data*, CMS-PAS-JME-16-003 (2016).

[40] J. Thaler and K. Van Tilburg, *Maximizing boosted top identification by minimizing N-subjettiness*, *JHEP* **02** (2012) 093 [arXiv:1108.2701] [INSPIRE].

[41] M. Dasgupta, A. Fregoso, S. Marzani and G.P. Salam, *Towards an understanding of jet substructure*, *JHEP* **09** (2013) 029 [arXiv:1307.0007] [INSPIRE].

[42] A.J. Larkoski, S. Marzani, G. Soyez and J. Thaler, *Soft drop*, *JHEP* **05** (2014) 146 [arXiv:1402.2657] [INSPIRE].

[43] CMS collaboration, *Identification of heavy-flavour jets with the CMS detector in pp collisions at 13 TeV*, 2018 *JINST* **13** P05011 [arXiv:1712.07158] [INSPIRE].

[44] CMS collaboration, *Search for massive resonances decaying into WW, WZ, ZZ, qW and qZ with dijet final states at $\sqrt{s} = 13$ TeV*, *Phys. Rev.* **D 97** (2018) 072006 [arXiv:1708.05379] [INSPIRE].

[45] CMS collaboration, *Measurement of differential cross sections for top quark pair production using the lepton+jets final state in proton-proton collisions at 13 TeV*, *Phys. Rev.* **D 95** (2017) 092001 [arXiv:1610.04191] [INSPIRE].

[46] J.S. Conway, *Incorporating nuisance parameters in likelihoods for multisource spectra*, in *Proceedings, PHYSTAT 2011 workshop on statistical issues related to discovery claims in search experiments and unfolding, CERN, Geneva, Switzerland 17–20 January 2011*, pp. 115–120, 2011, arXiv:1103.0354 [INSPIRE].

[47] CMS collaboration, *Measurement of the inelastic proton-proton cross section at $\sqrt{s} = 13$ TeV*, *JHEP* **07** (2018) 161 [arXiv:1802.02613] [INSPIRE].

[48] NNPDF collaboration, *Parton distributions from high-precision collider data*, *Eur. Phys. J.* **C 77** (2017) 663 [arXiv:1706.00428] [INSPIRE].

[49] R.J. Barlow and C. Beeston, *Fitting using finite Monte Carlo samples*, *Comput. Phys. Commun.* **77** (1993) 219 [INSPIRE].

JHEP03(2019)127

The CMS collaboration

Yerevan Physics Institute, Yerevan, Armenia

A.M. Sirunyan, A. Tumasyan

Institut für Hochenergiephysik, Wien, Austria

W. Adam, F. Ambrogi, E. Asilar, T. Bergauer, J. Brandstetter, M. Dragicevic, J. Erö, A. Escalante Del Valle, M. Flechl, R. Frühwirth[1], V.M. Ghete, J. Hrubec, M. Jeitler[1], N. Krammer, I. Krätschmer, D. Liko, T. Madlener, I. Mikulec, N. Rad, H. Rohringer, J. Schieck[1], R. Schöfbeck, M. Spanring, D. Spitzbart, A. Taurok, W. Waltenberger, J. Wittmann, C.-E. Wulz[1], M. Zarucki

Institute for Nuclear Problems, Minsk, Belarus

V. Chekhovsky, V. Mossolov, J. Suarez Gonzalez

Universiteit Antwerpen, Antwerpen, Belgium

E.A. De Wolf, D. Di Croce, X. Janssen, J. Lauwers, M. Pieters, H. Van Haevermaet, P. Van Mechelen, N. Van Remortel

Vrije Universiteit Brussel, Brussel, Belgium

S. Abu Zeid, F. Blekman, J. D'Hondt, J. De Clercq, K. Deroover, G. Flouris, D. Lontkovskyi, S. Lowette, I. Marchesini, S. Moortgat, L. Moreels, Q. Python, K. Skovpen, S. Tavernier, W. Van Doninck, P. Van Mulders, I. Van Parijs

Université Libre de Bruxelles, Bruxelles, Belgium

D. Beghin, B. Bilin, H. Brun, B. Clerbaux, G. De Lentdecker, H. Delannoy, B. Dorney, G. Fasanella, L. Favart, R. Goldouzian, A. Grebenyuk, A.K. Kalsi, T. Lenzi, J. Luetic, N. Postiau, E. Starling, L. Thomas, C. Vander Velde, P. Vanlaer, D. Vannerom, Q. Wang

Ghent University, Ghent, Belgium

T. Cornelis, D. Dobur, A. Fagot, M. Gul, I. Khvastunov[2], D. Poyraz, C. Roskas, D. Trocino, M. Tytgat, W. Verbeke, B. Vermassen, M. Vit, N. Zaganidis

Université Catholique de Louvain, Louvain-la-Neuve, Belgium

H. Bakhshiansohi, O. Bondu, S. Brochet, G. Bruno, C. Caputo, P. David, C. Delaere, M. Delcourt, A. Giammanco, G. Krintiras, V. Lemaitre, A. Magitteri, K. Piotrzkowski, A. Saggio, M. Vidal Marono, P. Vischia, S. Wertz, J. Zobec

Centro Brasileiro de Pesquisas Fisicas, Rio de Janeiro, Brazil

F.L. Alves, G.A. Alves, M. Correa Martins Junior, G. Correia Silva, C. Hensel, A. Moraes, M.E. Pol, P. Rebello Teles

Universidade do Estado do Rio de Janeiro, Rio de Janeiro, Brazil

E. Belchior Batista Das Chagas, W. Carvalho, J. Chinellato[3], E. Coelho, E.M. Da Costa, G.G. Da Silveira[4], D. De Jesus Damiao, C. De Oliveira Martins, S. Fonseca De Souza, H. Malbouisson, D. Matos Figueiredo, M. Melo De Almeida, C. Mora Herrera, L. Mundim, H. Nogima, W.L. Prado Da Silva, L.J. Sanchez Rosas, A. Santoro, A. Sznajder, M. Thiel, E.J. Tonelli Manganote[3], F. Torres Da Silva De Araujo, A. Vilela Pereira

JHEP03(2019)127

Universidade Estadual Paulista [a], Universidade Federal do ABC [b], São Paulo, Brazil

S. Ahuja[a], C.A. Bernardes[a], L. Calligaris[a], T.R. Fernandez Perez Tomei[a], E.M. Gregores[b], P.G. Mercadante[b], S.F. Novaes[a], SandraS. Padula[a]

Institute for Nuclear Research and Nuclear Energy, Bulgarian Academy of Sciences, Sofia, Bulgaria

A. Aleksandrov, R. Hadjiiska, P. Iaydjiev, A. Marinov, M. Misheva, M. Rodozov, M. Shopova, G. Sultanov

University of Sofia, Sofia, Bulgaria

A. Dimitrov, L. Litov, B. Pavlov, P. Petkov

Beihang University, Beijing, China

W. Fang[5], X. Gao[5], L. Yuan

Institute of High Energy Physics, Beijing, China

M. Ahmad, J.G. Bian, G.M. Chen, H.S. Chen, M. Chen, Y. Chen, C.H. Jiang, D. Leggat, H. Liao, Z. Liu, S.M. Shaheen[6], A. Spiezia, J. Tao, Z. Wang, E. Yazgan, H. Zhang, S. Zhang[6], J. Zhao

State Key Laboratory of Nuclear Physics and Technology, Peking University, Beijing, China

Y. Ban, G. Chen, A. Levin, J. Li, L. Li, Q. Li, Y. Mao, S.J. Qian, D. Wang

Tsinghua University, Beijing, China

Y. Wang

Universidad de Los Andes, Bogota, Colombia

C. Avila, A. Cabrera, C.A. Carrillo Montoya, L.F. Chaparro Sierra, C. Florez, C.F. González Hernández, M.A. Segura Delgado

University of Split, Faculty of Electrical Engineering, Mechanical Engineering and Naval Architecture, Split, Croatia

B. Courbon, N. Godinovic, D. Lelas, I. Puljak, T. Sculac

University of Split, Faculty of Science, Split, Croatia

Z. Antunovic, M. Kovac

Institute Rudjer Boskovic, Zagreb, Croatia

V. Brigljevic, D. Ferencek, K. Kadija, B. Mesic, A. Starodumov[7], T. Susa

University of Cyprus, Nicosia, Cyprus

M.W. Ather, A. Attikis, M. Kolosova, G. Mavromanolakis, J. Mousa, C. Nicolaou, F. Ptochos, P.A. Razis, H. Rykaczewski

Charles University, Prague, Czech Republic

M. Finger[8], M. Finger Jr.[8]

JHEP03(2019)127

Escuela Politecnica Nacional, Quito, Ecuador

E. Ayala

Universidad San Francisco de Quito, Quito, Ecuador

E. Carrera Jarrin

Academy of Scientific Research and Technology of the Arab Republic of Egypt, Egyptian Network of High Energy Physics, Cairo, Egypt

M.A. Mahmoud[9,10], Y. Mohammed[9], E. Salama[10,11]

National Institute of Chemical Physics and Biophysics, Tallinn, Estonia

S. Bhowmik, A. Carvalho Antunes De Oliveira, R.K. Dewanjee, K. Ehataht, M. Kadastik, M. Raidal, C. Veelken

Department of Physics, University of Helsinki, Helsinki, Finland

P. Eerola, H. Kirschenmann, J. Pekkanen, M. Voutilainen

Helsinki Institute of Physics, Helsinki, Finland

J. Havukainen, J.K. Heikkilä, T. Järvinen, V. Karimäki, R. Kinnunen, T. Lampén, K. Lassila-Perini, S. Laurila, S. Lehti, T. Lindén, P. Luukka, T. Mäenpää, H. Siikonen, E. Tuominen, J. Tuominiemi

Lappeenranta University of Technology, Lappeenranta, Finland

T. Tuuva

IRFU, CEA, Université Paris-Saclay, Gif-sur-Yvette, France

M. Besancon, F. Couderc, M. Dejardin, D. Denegri, J.L. Faure, F. Ferri, S. Ganjour, A. Givernaud, P. Gras, G. Hamel de Monchenault, P. Jarry, C. Leloup, E. Locci, J. Malcles, G. Negro, J. Rander, A. Rosowsky, M.Ö. Sahin, M. Titov

Laboratoire Leprince-Ringuet, Ecole polytechnique, CNRS/IN2P3, Université Paris-Saclay, Palaiseau, France

A. Abdulsalam[12], C. Amendola, I. Antropov, F. Beaudette, P. Busson, C. Charlot, R. Granier de Cassagnac, I. Kucher, A. Lobanov, J. Martin Blanco, C. Martin Perez, M. Nguyen, C. Ochando, G. Ortona, P. Paganini, P. Pigard, J. Rembser, R. Salerno, J.B. Sauvan, Y. Sirois, A.G. Stahl Leiton, A. Zabi, A. Zghiche

Université de Strasbourg, CNRS, IPHC UMR 7178, Strasbourg, France

J.-L. Agram[13], J. Andrea, D. Bloch, J.-M. Brom, E.C. Chabert, V. Cherepanov, C. Collard, E. Conte[13], J.-C. Fontaine[13], D. Gelé, U. Goerlach, M. Jansová, A.-C. Le Bihan, N. Tonon, P. Van Hove

Centre de Calcul de l'Institut National de Physique Nucleaire et de Physique des Particules, CNRS/IN2P3, Villeurbanne, France

S. Gadrat

JHEP03(2019)127

Université de Lyon, Université Claude Bernard Lyon 1, CNRS-IN2P3, Institut de Physique Nucléaire de Lyon, Villeurbanne, France
S. Beauceron, C. Bernet, G. Boudoul, N. Chanon, R. Chierici, D. Contardo, P. Depasse, H. El Mamouni, J. Fay, L. Finco, S. Gascon, M. Gouzevitch, G. Grenier, B. Ille, F. Lagarde, I.B. Laktineh, H. Lattaud, M. Lethuillier, L. Mirabito, S. Perries, A. Popov[14], V. Sordini, G. Touquet, M. Vander Donckt, S. Viret

Georgian Technical University, Tbilisi, Georgia
T. Toriashvili[15]

Tbilisi State University, Tbilisi, Georgia
Z. Tsamalaidze[8]

RWTH Aachen University, I. Physikalisches Institut, Aachen, Germany
C. Autermann, L. Feld, M.K. Kiesel, K. Klein, M. Lipinski, M. Preuten, M.P. Rauch, C. Schomakers, J. Schulz, M. Teroerde, B. Wittmer

RWTH Aachen University, III. Physikalisches Institut A, Aachen, Germany
A. Albert, D. Duchardt, M. Erdmann, S. Erdweg, T. Esch, R. Fischer, S. Ghosh, A. Güth, T. Hebbeker, C. Heidemann, K. Hoepfner, H. Keller, L. Mastrolorenzo, M. Merschmeyer, A. Meyer, P. Millet, S. Mukherjee, T. Pook, M. Radziej, H. Reithler, M. Rieger, A. Schmidt, D. Teyssier, S. Thüer

RWTH Aachen University, III. Physikalisches Institut B, Aachen, Germany
G. Flügge, O. Hlushchenko, T. Kress, T. Müller, A. Nehrkorn, A. Nowack, C. Pistone, O. Pooth, D. Roy, H. Sert, A. Stahl[16]

Deutsches Elektronen-Synchrotron, Hamburg, Germany
M. Aldaya Martin, T. Arndt, C. Asawatangtrakuldee, I. Babounikau, K. Beernaert, O. Behnke, U. Behrens, A. Bermúdez Martínez, D. Bertsche, A.A. Bin Anuar, K. Borras[17], V. Botta, A. Campbell, P. Connor, C. Contreras-Campana, V. Danilov, A. De Wit, M.M. Defranchis, C. Diez Pardos, D. Domínguez Damiani, G. Eckerlin, T. Eichhorn, A. Elwood, E. Eren, E. Gallo[18], A. Geiser, J.M. Grados Luyando, A. Grohsjean, M. Guthoff, M. Haranko, A. Harb, H. Jung, M. Kasemann, J. Keaveney, C. Kleinwort, J. Knolle, D. Krücker, W. Lange, A. Lelek, T. Lenz, J. Leonard, K. Lipka, W. Lohmann[19], R. Mankel, I.-A. Melzer-Pellmann, A.B. Meyer, M. Meyer, M. Missiroli, J. Mnich, V. Myronenko, S.K. Pflitsch, D. Pitzl, A. Raspereza, P. Saxena, P. Schütze, C. Schwanenberger, R. Shevchenko, A. Singh, H. Tholen, O. Turkot, A. Vagnerini, G.P. Van Onsem, R. Walsh, Y. Wen, K. Wichmann, C. Wissing, O. Zenaiev

University of Hamburg, Hamburg, Germany
R. Aggleton, S. Bein, L. Benato, A. Benecke, V. Blobel, T. Dreyer, A. Ebrahimi, E. Garutti, D. Gonzalez, P. Gunnellini, J. Haller, A. Hinzmann, A. Karavdina, G. Kasieczka, R. Klanner, R. Kogler, N. Kovalchuk, S. Kurz, V. Kutzner, J. Lange, D. Marconi, J. Multhaup, M. Niedziela, C.E.N. Niemeyer, D. Nowatschin, A. Perieanu, A. Reimers, O. Rieger, C. Scharf, P. Schleper, S. Schumann, J. Schwandt, J. Sonneveld, H. Stadie, G. Steinbrück, F.M. Stober, M. Stöver, A. Vanhoefer, B. Vormwald, I. Zoi

JHEP03(2019)127

Karlsruher Institut fuer Technologie, Karlsruhe, Germany
M. Akbiyik, C. Barth, M. Baselga, S. Baur, E. Butz, R. Caspart, T. Chwalek, F. Colombo, W. De Boer, A. Dierlamm, K. El Morabit, N. Faltermann, B. Freund, M. Giffels, M.A. Harrendorf, F. Hartmann[16], S.M. Heindl, U. Husemann, I. Katkov[14], S. Kudella, S. Mitra, M.U. Mozer, Th. Müller, M. Musich, M. Plagge, G. Quast, K. Rabbertz, M. Schröder, I. Shvetsov, H.J. Simonis, R. Ulrich, S. Wayand, M. Weber, T. Weiler, C. Wöhrmann, R. Wolf

Institute of Nuclear and Particle Physics (INPP), NCSR Demokritos, Aghia Paraskevi, Greece
G. Anagnostou, G. Daskalakis, T. Geralis, A. Kyriakis, D. Loukas, G. Paspalaki

National and Kapodistrian University of Athens, Athens, Greece
A. Agapitos, G. Karathanasis, P. Kontaxakis, A. Panagiotou, I. Papavergou, N. Saoulidou, E. Tziaferi, K. Vellidis

National Technical University of Athens, Athens, Greece
K. Kousouris, I. Papakrivopoulos, G. Tsipolitis

University of Ioánnina, Ioánnina, Greece
I. Evangelou, C. Foudas, P. Gianneios, P. Katsoulis, P. Kokkas, S. Mallios, N. Manthos, I. Papadopoulos, E. Paradas, J. Strologas, F.A. Triantis, D. Tsitsonis

MTA-ELTE Lendület CMS Particle and Nuclear Physics Group, Eötvös Loránd University, Budapest, Hungary
M. Bartók[20], M. Csanad, N. Filipovic, P. Major, M.I. Nagy, G. Pasztor, O. Surányi, G.I. Veres

Wigner Research Centre for Physics, Budapest, Hungary
G. Bencze, C. Hajdu, D. Horvath[21], Á. Hunyadi, F. Sikler, T.Á. Vámi, V. Veszpremi, G. Vesztergombi[†]

Institute of Nuclear Research ATOMKI, Debrecen, Hungary
N. Beni, S. Czellar, J. Karancsi[20], A. Makovec, J. Molnar, Z. Szillasi

Institute of Physics, University of Debrecen, Debrecen, Hungary
P. Raics, Z.L. Trocsanyi, B. Ujvari

Indian Institute of Science (IISc), Bangalore, India
S. Choudhury, J.R. Komaragiri, P.C. Tiwari

National Institute of Science Education and Research, HBNI, Bhubaneswar, India
S. Bahinipati[23], C. Kar, P. Mal, K. Mandal, A. Nayak[24], D.K. Sahoo[23], S.K. Swain

Panjab University, Chandigarh, India
S. Bansal, S.B. Beri, V. Bhatnagar, S. Chauhan, R. Chawla, N. Dhingra, R. Gupta, A. Kaur, M. Kaur, S. Kaur, P. Kumari, M. Lohan, A. Mehta, K. Sandeep, S. Sharma, J.B. Singh, A.K. Virdi, G. Walia

JHEP03(2019)127

University of Delhi, Delhi, India

A. Bhardwaj, B.C. Choudhary, R.B. Garg, M. Gola, S. Keshri, Ashok Kumar, S. Malhotra, M. Naimuddin, P. Priyanka, K. Ranjan, Aashaq Shah, R. Sharma

Saha Institute of Nuclear Physics, HBNI, Kolkata, India

R. Bhardwaj[25], M. Bharti[25], R. Bhattacharya, S. Bhattacharya, U. Bhawandeep[25], D. Bhowmik, S. Dey, S. Dutt[25], S. Dutta, S. Ghosh, K. Mondal, S. Nandan, A. Purohit, P.K. Rout, A. Roy, S. Roy Chowdhury, G. Saha, S. Sarkar, M. Sharan, B. Singh[25], S. Thakur[25]

Indian Institute of Technology Madras, Madras, India

P.K. Behera

Bhabha Atomic Research Centre, Mumbai, India

R. Chudasama, D. Dutta, V. Jha, V. Kumar, D.K. Mishra, P.K. Netrakanti, L.M. Pant, P. Shukla

Tata Institute of Fundamental Research-A, Mumbai, India

T. Aziz, M.A. Bhat, S. Dugad, G.B. Mohanty, N. Sur, B. Sutar, RavindraKumar Verma

Tata Institute of Fundamental Research-B, Mumbai, India

S. Banerjee, S. Bhattacharya, S. Chatterjee, P. Das, M. Guchait, Sa. Jain, S. Karmakar, S. Kumar, M. Maity[26], G. Majumder, K. Mazumdar, N. Sahoo, T. Sarkar[26]

Indian Institute of Science Education and Research (IISER), Pune, India

S. Chauhan, S. Dube, V. Hegde, A. Kapoor, K. Kothekar, S. Pandey, A. Rane, A. Rastogi, S. Sharma

Institute for Research in Fundamental Sciences (IPM), Tehran, Iran

S. Chenarani[27], E. Eskandari Tadavani, S.M. Etesami[27], M. Khakzad, M. Mohammadi Najafabadi, M. Naseri, F. Rezaei Hosseinabadi, B. Safarzadeh[28], M. Zeinali

University College Dublin, Dublin, Ireland

M. Felcini, M. Grunewald

INFN Sezione di Bari [a], Università di Bari [b], Politecnico di Bari [c], Bari, Italy

M. Abbrescia[a,b], C. Calabria[a,b], A. Colaleo[a], D. Creanza[a,c], L. Cristella[a,b], N. De Filippis[a,c], M. De Palma[a,b], A. Di Florio[a,b], F. Errico[a,b], L. Fiore[a], A. Gelmi[a,b], G. Iaselli[a,c], M. Ince[a,b], S. Lezki[a,b], G. Maggi[a,c], M. Maggi[a], G. Miniello[a,b], S. My[a,b], S. Nuzzo[a,b], A. Pompili[a,b], G. Pugliese[a,c], R. Radogna[a], A. Ranieri[a], G. Selvaggi[a,b], A. Sharma[a], L. Silvestris[a], R. Venditti[a], P. Verwilligen[a], G. Zito[a]

INFN Sezione di Bologna [a], Università di Bologna [b], Bologna, Italy

G. Abbiendi[a], C. Battilana[a,b], D. Bonacorsi[a,b], L. Borgonovi[a,b], S. Braibant-Giacomelli[a,b], R. Campanini[a,b], P. Capiluppi[a,b], A. Castro[a,b], F.R. Cavallo[a], S.S. Chhibra[a,b], C. Ciocca[a], G. Codispoti[a,b], M. Cuffiani[a,b], G.M. Dallavalle[a], F. Fabbri[a], A. Fanfani[a,b], E. Fontanesi, P. Giacomelli[a], C. Grandi[a], L. Guiducci[a,b], F. Iemmi[a,b], S. Lo Meo[a], S. Marcellini[a], G. Masetti[a], A. Montanari[a], F.L. Navarria[a,b], A. Perrotta[a], F. Primavera[a,b,16], T. Rovelli[a,b], G.P. Siroli[a,b], N. Tosi[a]

JHEP03(2019)127

INFN Sezione di Catania [a], Università di Catania [b], Catania, Italy

S. Albergo[a,b], A. Di Mattia[a], R. Potenza[a,b], A. Tricomi[a,b], C. Tuve[a,b]

INFN Sezione di Firenze [a], Università di Firenze [b], Firenze, Italy

G. Barbagli[a], K. Chatterjee[a,b], V. Ciulli[a,b], C. Civinini[a], R. D'Alessandro[a,b], E. Focardi[a,b], G. Latino, P. Lenzi[a,b], M. Meschini[a], S. Paoletti[a], L. Russo[a,29], G. Sguazzoni[a], D. Strom[a], L. Viliani[a]

INFN Laboratori Nazionali di Frascati, Frascati, Italy

L. Benussi, S. Bianco, F. Fabbri, D. Piccolo

INFN Sezione di Genova [a], Università di Genova [b], Genova, Italy

F. Ferro[a], R. Mulargia[a,b], F. Ravera[a,b], E. Robutti[a], S. Tosi[a,b]

INFN Sezione di Milano-Bicocca [a], Università di Milano-Bicocca [b], Milano, Italy

A. Benaglia[a], A. Beschi[b], F. Brivio[a,b], V. Ciriolo[a,b,16], S. Di Guida[a,d,16], M.E. Dinardo[a,b], S. Fiorendi[a,b], S. Gennai[a], A. Ghezzi[a,b], P. Govoni[a,b], M. Malberti[a,b], S. Malvezzi[a], D. Menasce[a], F. Monti, L. Moroni[a], M. Paganoni[a,b], D. Pedrini[a], S. Ragazzi[a,b], T. Tabarelli de Fatis[a,b], D. Zuolo[a,b]

INFN Sezione di Napoli [a], Università di Napoli 'Federico II' [b], Napoli, Italy, Università della Basilicata [c], Potenza, Italy, Università G. Marconi [d], Roma, Italy

S. Buontempo[a], N. Cavallo[a,c], A. De Iorio[a,b], A. Di Crescenzo[a,b], F. Fabozzi[a,c], F. Fienga[a], G. Galati[a], A.O.M. Iorio[a,b], W.A. Khan[a], L. Lista[a], S. Meola[a,d,16], P. Paolucci[a,16], C. Sciacca[a,b], E. Voevodina[a,b]

INFN Sezione di Padova [a], Università di Padova [b], Padova, Italy, Università di Trento [c], Trento, Italy

P. Azzi[a], N. Bacchetta[a], D. Bisello[a,b], A. Boletti[a,b], A. Bragagnolo, R. Carlin[a,b], P. Checchia[a], M. Dall'Osso[a,b], P. De Castro Manzano[a], T. Dorigo[a], U. Dosselli[a], F. Gasparini[a,b], U. Gasparini[a,b], A. Gozzelino[a], S.Y. Hoh, S. Lacaprara[a], P. Lujan, M. Margoni[a,b], A.T. Meneguzzo[a,b], J. Pazzini[a,b], M. Presilla[b], P. Ronchese[a,b], R. Rossin[a,b], F. Simonetto[a,b], A. Tiko, E. Torassa[a], M. Tosi[a,b], M. Zanetti[a,b], P. Zotto[a,b], G. Zumerle[a,b]

INFN Sezione di Pavia [a], Università di Pavia [b], Pavia, Italy

A. Braghieri[a], A. Magnani[a], P. Montagna[a,b], S.P. Ratti[a,b], V. Re[a], M. Ressegotti[a,b], C. Riccardi[a,b], P. Salvini[a], I. Vai[a,b], P. Vitulo[a,b]

INFN Sezione di Perugia [a], Università di Perugia [b], Perugia, Italy

M. Biasini[a,b], G.M. Bilei[a], C. Cecchi[a,b], D. Ciangottini[a,b], L. Fanò[a,b], P. Lariccia[a,b], R. Leonardi[a,b], E. Manoni[a], G. Mantovani[a,b], V. Mariani[a,b], M. Menichelli[a], A. Rossi[a,b], A. Santocchia[a,b], D. Spiga[a]

JHEP03(2019)127

INFN Sezione di Pisa [a], Università di Pisa [b], Scuola Normale Superiore di Pisa [c], Pisa, Italy

K. Androsov[a], P. Azzurri[a], G. Bagliesi[a], L. Bianchini[a], T. Boccali[a], L. Borrello, R. Castaldi[a], M.A. Ciocci[a,b], R. Dell'Orso[a], G. Fedi[a], F. Fiori[a,c], L. Giannini[a,c], A. Giassi[a], M.T. Grippo[a], F. Ligabue[a,c], E. Manca[a,c], G. Mandorli[a,c], A. Messineo[a,b], F. Palla[a], A. Rizzi[a,b], G. Rolandi[30], P. Spagnolo[a], R. Tenchini[a], G. Tonelli[a,b], A. Venturi[a], P.G. Verdini[a]

INFN Sezione di Roma [a], Sapienza Università di Roma [b], Rome, Italy

L. Barone[a,b], F. Cavallari[a], M. Cipriani[a,b], D. Del Re[a,b], E. Di Marco[a,b], M. Diemoz[a], S. Gelli[a,b], E. Longo[a,b], B. Marzocchi[a,b], P. Meridiani[a], G. Organtini[a,b], F. Pandolfi[a], R. Paramatti[a,b], F. Preiato[a,b], S. Rahatlou[a,b], C. Rovelli[a], F. Santanastasio[a,b]

INFN Sezione di Torino [a], Università di Torino [b], Torino, Italy, Università del Piemonte Orientale [c], Novara, Italy

N. Amapane[a,b], R. Arcidiacono[a,c], S. Argiro[a,b], M. Arneodo[a,c], N. Bartosik[a], R. Bellan[a,b], C. Biino[a], A. Cappati[a,b], N. Cartiglia[a], F. Cenna[a,b], S. Cometti[a], M. Costa[a,b], R. Covarelli[a,b], N. Demaria[a], B. Kiani[a,b], C. Mariotti[a], S. Maselli[a], E. Migliore[a,b], V. Monaco[a,b], E. Monteil[a,b], M. Monteno[a], M.M. Obertino[a,b], L. Pacher[a,b], N. Pastrone[a], M. Pelliccioni[a], G.L. Pinna Angioni[a,b], A. Romero[a,b], M. Ruspa[a,c], R. Sacchi[a,b], R. Salvatico[a,b], K. Shchelina[a,b], V. Sola[a], A. Solano[a,b], D. Soldi[a,b], A. Staiano[a]

INFN Sezione di Trieste [a], Università di Trieste [b], Trieste, Italy

S. Belforte[a], V. Candelise[a,b], M. Casarsa[a], F. Cossutti[a], A. Da Rold[a,b], G. Della Ricca[a,b], F. Vazzoler[a,b], A. Zanetti[a]

Kyungpook National University, Daegu, Korea

D.H. Kim, G.N. Kim, M.S. Kim, J. Lee, S. Lee, S.W. Lee, C.S. Moon, Y.D. Oh, S.I. Pak, S. Sekmen, D.C. Son, Y.C. Yang

Chonnam National University, Institute for Universe and Elementary Particles, Kwangju, Korea

H. Kim, D.H. Moon, G. Oh

Hanyang University, Seoul, Korea

B. Francois, J. Goh[31], T.J. Kim

Korea University, Seoul, Korea

S. Cho, S. Choi, Y. Go, D. Gyun, S. Ha, B. Hong, Y. Jo, K. Lee, K.S. Lee, S. Lee, J. Lim, S.K. Park, Y. Roh

Sejong University, Seoul, Korea

H.S. Kim

Seoul National University, Seoul, Korea

J. Almond, J. Kim, J.S. Kim, H. Lee, K. Lee, K. Nam, S.B. Oh, B.C. Radburn-Smith, S.h. Seo, U.K. Yang, H.D. Yoo, G.B. Yu

JHEP03(2019)127

University of Seoul, Seoul, Korea
D. Jeon, H. Kim, J.H. Kim, J.S.H. Lee, I.C. Park

Sungkyunkwan University, Suwon, Korea
Y. Choi, C. Hwang, J. Lee, I. Yu

Vilnius University, Vilnius, Lithuania
V. Dudenas, A. Juodagalvis, J. Vaitkus

National Centre for Particle Physics, Universiti Malaya, Kuala Lumpur, Malaysia
I. Ahmed, Z.A. Ibrahim, M.A.B. Md Ali[32], F. Mohamad Idris[33], W.A.T. Wan Abdullah, M.N. Yusli, Z. Zolkapli

Universidad de Sonora (UNISON), Hermosillo, Mexico
J.F. Benitez, A. Castaneda Hernandez, J.A. Murillo Quijada

Centro de Investigacion y de Estudios Avanzados del IPN, Mexico City, Mexico
H. Castilla-Valdez, E. De La Cruz-Burelo, M.C. Duran-Osuna, I. Heredia-De La Cruz[34], R. Lopez-Fernandez, J. Mejia Guisao, R.I. Rabadan-Trejo, M. Ramirez-Garcia, G. Ramirez-Sanchez, R. Reyes-Almanza, A. Sanchez-Hernandez

Universidad Iberoamericana, Mexico City, Mexico
S. Carrillo Moreno, C. Oropeza Barrera, F. Vazquez Valencia

Benemerita Universidad Autonoma de Puebla, Puebla, Mexico
J. Eysermans, I. Pedraza, H.A. Salazar Ibarguen, C. Uribe Estrada

Universidad Autónoma de San Luis Potosí, San Luis Potosí, Mexico
A. Morelos Pineda

University of Auckland, Auckland, New Zealand
D. Krofcheck

University of Canterbury, Christchurch, New Zealand
S. Bheesette, P.H. Butler

National Centre for Physics, Quaid-I-Azam University, Islamabad, Pakistan
A. Ahmad, M. Ahmad, M.I. Asghar, Q. Hassan, H.R. Hoorani, A. Saddique, M.A. Shah, M. Shoaib, M. Waqas

National Centre for Nuclear Research, Swierk, Poland
H. Bialkowska, M. Bluj, B. Boimska, T. Frueboes, M. Górski, M. Kazana, M. Szleper, P. Traczyk, P. Zalewski

Institute of Experimental Physics, Faculty of Physics, University of Warsaw, Warsaw, Poland
K. Bunkowski, A. Byszuk[35], K. Doroba, A. Kalinowski, M. Konecki, J. Krolikowski, M. Misiura, M. Olszewski, A. Pyskir, M. Walczak

JHEP03(2019)127

Laboratório de Instrumentação e Física Experimental de Partículas, Lisboa, Portugal

M. Araujo, P. Bargassa, C. Beirão Da Cruz E Silva, A. Di Francesco, P. Faccioli, B. Galinhas, M. Gallinaro, J. Hollar, N. Leonardo, J. Seixas, G. Strong, O. Toldaiev, J. Varela

Joint Institute for Nuclear Research, Dubna, Russia

S. Afanasiev, P. Bunin, M. Gavrilenko, I. Golutvin, I. Gorbunov, A. Kamenev, V. Karjavine, A. Lanev, A. Malakhov, V. Matveev[36,37], P. Moisenz, V. Palichik, V. Perelygin, S. Shmatov, S. Shulha, N. Skatchkov, V. Smirnov, N. Voytishin, A. Zarubin

Petersburg Nuclear Physics Institute, Gatchina (St. Petersburg), Russia

V. Golovtsov, Y. Ivanov, V. Kim[38], E. Kuznetsova[39], P. Levchenko, V. Murzin, V. Oreshkin, I. Smirnov, D. Sosnov, V. Sulimov, L. Uvarov, S. Vavilov, A. Vorobyev

Institute for Nuclear Research, Moscow, Russia

Yu. Andreev, A. Dermenev, S. Gninenko, N. Golubev, A. Karneyeu, M. Kirsanov, N. Krasnikov, A. Pashenkov, D. Tlisov, A. Toropin

Institute for Theoretical and Experimental Physics, Moscow, Russia

V. Epshteyn, V. Gavrilov, N. Lychkovskaya, V. Popov, I. Pozdnyakov, G. Safronov, A. Spiridonov, A. Stepennov, V. Stolin, M. Toms, E. Vlasov, A. Zhokin

Moscow Institute of Physics and Technology, Moscow, Russia

T. Aushev

National Research Nuclear University 'Moscow Engineering Physics Institute' (MEPhI), Moscow, Russia

R. Chistov[40], M. Danilov[40], P. Parygin, D. Philippov, S. Polikarpov[40], E. Tarkovskii

P.N. Lebedev Physical Institute, Moscow, Russia

V. Andreev, M. Azarkin, I. Dremin[37], M. Kirakosyan, A. Terkulov

Skobeltsyn Institute of Nuclear Physics, Lomonosov Moscow State University, Moscow, Russia

A. Baskakov, A. Belyaev, E. Boos, V. Bunichev, M. Dubinin[41], L. Dudko, A. Ershov, V. Klyukhin, O. Kodolova, I. Lokhtin, I. Miagkov, S. Obraztsov, M. Perfilov, S. Petrushanko, V. Savrin

Novosibirsk State University (NSU), Novosibirsk, Russia

A. Barnyakov[42], V. Blinov[42], T. Dimova[42], L. Kardapoltsev[42], Y. Skovpen[42]

Institute for High Energy Physics of National Research Centre 'Kurchatov Institute', Protvino, Russia

I. Azhgirey, I. Bayshev, S. Bitioukov, V. Kachanov, A. Kalinin, D. Konstantinov, P. Mandrik, V. Petrov, R. Ryutin, S. Slabospitskii, A. Sobol, S. Troshin, N. Tyurin, A. Uzunian, A. Volkov

JHEP03(2019)127

National Research Tomsk Polytechnic University, Tomsk, Russia
A. Babaev, S. Baidali, V. Okhotnikov

University of Belgrade, Faculty of Physics and Vinca Institute of Nuclear Sciences, Belgrade, Serbia
P. Adzic[43], P. Cirkovic, D. Devetak, M. Dordevic, J. Milosevic

Centro de Investigaciones Energéticas Medioambientales y Tecnológicas (CIEMAT), Madrid, Spain
J. Alcaraz Maestre, A. Álvarez Fernández, I. Bachiller, M. Barrio Luna, J.A. Brochero Cifuentes, M. Cerrada, N. Colino, B. De La Cruz, A. Delgado Peris, C. Fernandez Bedoya, J.P. Fernández Ramos, J. Flix, M.C. Fouz, O. Gonzalez Lopez, S. Goy Lopez, J.M. Hernandez, M.I. Josa, D. Moran, A. Pérez-Calero Yzquierdo, J. Puerta Pelayo, I. Redondo, L. Romero, M.S. Soares, A. Triossi

Universidad Autónoma de Madrid, Madrid, Spain
C. Albajar, J.F. de Trocóniz

Universidad de Oviedo, Oviedo, Spain
J. Cuevas, C. Erice, J. Fernandez Menendez, S. Folgueras, I. Gonzalez Caballero, J.R. González Fernández, E. Palencia Cortezon, V. Rodríguez Bouza, S. Sanchez Cruz, J.M. Vizan Garcia

Instituto de Física de Cantabria (IFCA), CSIC-Universidad de Cantabria, Santander, Spain
I.J. Cabrillo, A. Calderon, B. Chazin Quero, J. Duarte Campderros, M. Fernandez, P.J. Fernández Manteca, A. García Alonso, J. Garcia-Ferrero, G. Gomez, A. Lopez Virto, J. Marco, C. Martinez Rivero, P. Martinez Ruiz del Arbol, F. Matorras, J. Piedra Gomez, C. Prieels, T. Rodrigo, A. Ruiz-Jimeno, L. Scodellaro, N. Trevisani, I. Vila, R. Vilar Cortabitarte

University of Ruhuna, Department of Physics, Matara, Sri Lanka
N. Wickramage

CERN, European Organization for Nuclear Research, Geneva, Switzerland
D. Abbaneo, B. Akgun, E. Auffray, G. Auzinger, P. Baillon, A.H. Ball, D. Barney, J. Bendavid, M. Bianco, A. Bocci, C. Botta, E. Brondolin, T. Camporesi, M. Cepeda, G. Cerminara, E. Chapon, Y. Chen, G. Cucciati, D. d'Enterria, A. Dabrowski, N. Daci, V. Daponte, A. David, A. De Roeck, N. Deelen, M. Dobson, M. Dünser, N. Dupont, A. Elliott-Peisert, P. Everaerts, F. Fallavollita[44], D. Fasanella, G. Franzoni, J. Fulcher, W. Funk, D. Gigi, A. Gilbert, K. Gill, F. Glege, M. Gruchala, M. Guilbaud, D. Gulhan, J. Hegeman, C. Heidegger, V. Innocente, A. Jafari, P. Janot, O. Karacheban[19], J. Kieseler, A. Kornmayer, M. Krammer[1], C. Lange, P. Lecoq, C. Lourenço, L. Malgeri, M. Mannelli, A. Massironi, F. Meijers, J.A. Merlin, S. Mersi, E. Meschi, P. Milenovic[45], F. Moortgat, M. Mulders, J. Ngadiuba, S. Nourbakhsh, S. Orfanelli, L. Orsini, F. Pantaleo[16], L. Pape, E. Perez, M. Peruzzi, A. Petrilli, G. Petrucciani, A. Pfeiffer, M. Pierini, F.M. Pitters, D. Rabady, A. Racz, T. Reis, M. Rovere, H. Sakulin, C. Schäfer, C. Schwick, M. Selvaggi,

JHEP03(2019)127

A. Sharma, P. Silva, P. Sphicas[46], A. Stakia, J. Steggemann, D. Treille, A. Tsirou, V. Veckalns[47], M. Verzetti, W.D. Zeuner

Paul Scherrer Institut, Villigen, Switzerland

L. Caminada[48], K. Deiters, W. Erdmann, R. Horisberger, Q. Ingram, H.C. Kaestli, D. Kotlinski, U. Langenegger, T. Rohe, S.A. Wiederkehr

ETH Zurich - Institute for Particle Physics and Astrophysics (IPA), Zurich, Switzerland

M. Backhaus, L. Bäni, P. Berger, N. Chernyavskaya, G. Dissertori, M. Dittmar, M. Donegà, C. Dorfer, T.A. Gómez Espinosa, C. Grab, D. Hits, T. Klijnsma, W. Lustermann, R.A. Manzoni, M. Marionneau, M.T. Meinhard, F. Micheli, P. Musella, F. Nessi-Tedaldi, J. Pata, F. Pauss, G. Perrin, L. Perrozzi, S. Pigazzini, M. Quittnat, C. Reissel, D. Ruini, D.A. Sanz Becerra, M. Schönenberger, L. Shchutska, V.R. Tavolaro, K. Theofilatos, M.L. Vesterbacka Olsson, R. Wallny, D.H. Zhu

Universität Zürich, Zurich, Switzerland

T.K. Aarrestad, C. Amsler[49], D. Brzhechko, M.F. Canelli, A. De Cosa, R. Del Burgo, S. Donato, C. Galloni, T. Hreus, B. Kilminster, S. Leontsinis, I. Neutelings, G. Rauco, P. Robmann, D. Salerno, K. Schweiger, C. Seitz, Y. Takahashi, A. Zucchetta

National Central University, Chung-Li, Taiwan

T.H. Doan, R. Khurana, C.M. Kuo, W. Lin, A. Pozdnyakov, S.S. Yu

National Taiwan University (NTU), Taipei, Taiwan

P. Chang, Y. Chao, K.F. Chen, P.H. Chen, W.-S. Hou, Arun Kumar, Y.F. Liu, R.-S. Lu, E. Paganis, A. Psallidas, A. Steen

Chulalongkorn University, Faculty of Science, Department of Physics, Bangkok, Thailand

B. Asavapibhop, N. Srimanobhas, N. Suwonjandee

Çukurova University, Physics Department, Science and Art Faculty, Adana, Turkey

M.N. Bakirci[50], A. Bat, F. Boran, S. Cerci[51], S. Damarseckin, Z.S. Demiroglu, F. Dolek, C. Dozen, I. Dumanoglu, E. Eskut, S. Girgis, G. Gokbulut, Y. Guler, E. Gurpinar, I. Hos[52], C. Isik, E.E. Kangal[53], O. Kara, U. Kiminsu, M. Oglakci, G. Onengut, K. Ozdemir[54], A. Polatoz, D. Sunar Cerci[51], U.G. Tok, S. Turkcapar, I.S. Zorbakir, C. Zorbilmez

Middle East Technical University, Physics Department, Ankara, Turkey

B. Isildak[55], G. Karapinar[56], M. Yalvac, M. Zeyrek

Bogazici University, Istanbul, Turkey

I.O. Atakisi, E. Gülmez, M. Kaya[57], O. Kaya[58], S. Ozkorucuklu[59], S. Tekten, E.A. Yetkin[60]

Istanbul Technical University, Istanbul, Turkey

M.N. Agaras, A. Cakir, K. Cankocak, Y. Komurcu, S. Sen[61]

JHEP03(2019)127

Institute for Scintillation Materials of National Academy of Science of Ukraine, Kharkov, Ukraine

B. Grynyov

National Scientific Center, Kharkov Institute of Physics and Technology, Kharkov, Ukraine

L. Levchuk

University of Bristol, Bristol, United Kingdom

F. Ball, J.J. Brooke, D. Burns, E. Clement, D. Cussans, O. Davignon, H. Flacher, J. Goldstein, G.P. Heath, H.F. Heath, L. Kreczko, D.M. Newbold[62], S. Paramesvaran, B. Penning, T. Sakuma, D. Smith, V.J. Smith, J. Taylor, A. Titterton

Rutherford Appleton Laboratory, Didcot, United Kingdom

K.W. Bell, A. Belyaev[63], C. Brew, R.M. Brown, D. Cieri, D.J.A. Cockerill, J.A. Coughlan, K. Harder, S. Harper, J. Linacre, K. Manolopoulos, E. Olaiya, D. Petyt, C.H. Shepherd-Themistocleous, A. Thea, I.R. Tomalin, T. Williams, W.J. Womersley

Imperial College, London, United Kingdom

R. Bainbridge, P. Bloch, J. Borg, S. Breeze, O. Buchmuller, A. Bundock, D. Colling, P. Dauncey, G. Davies, M. Della Negra, R. Di Maria, G. Hall, G. Iles, T. James, M. Komm, C. Laner, L. Lyons, A.-M. Magnan, S. Malik, A. Martelli, J. Nash[64], A. Nikitenko[7], V. Palladino, M. Pesaresi, D.M. Raymond, A. Richards, A. Rose, E. Scott, C. Seez, A. Shtipliyski, G. Singh, M. Stoye, T. Strebler, S. Summers, A. Tapper, K. Uchida, T. Virdee[16], N. Wardle, D. Winterbottom, J. Wright, S.C. Zenz

Brunel University, Uxbridge, United Kingdom

J.E. Cole, P.R. Hobson, A. Khan, P. Kyberd, C.K. Mackay, A. Morton, I.D. Reid, L. Teodorescu, S. Zahid

Baylor University, Waco, USA

K. Call, J. Dittmann, K. Hatakeyama, H. Liu, C. Madrid, B. McMaster, N. Pastika, C. Smith

Catholic University of America, Washington, DC, USA

R. Bartek, A. Dominguez

The University of Alabama, Tuscaloosa, USA

A. Buccilli, S.I. Cooper, C. Henderson, P. Rumerio, C. West

Boston University, Boston, USA

D. Arcaro, T. Bose, D. Gastler, D. Pinna, D. Rankin, C. Richardson, J. Rohlf, L. Sulak, D. Zou

Brown University, Providence, USA

G. Benelli, X. Coubez, D. Cutts, M. Hadley, J. Hakala, U. Heintz, J.M. Hogan[65], K.H.M. Kwok, E. Laird, G. Landsberg, J. Lee, Z. Mao, M. Narain, S. Sagir[66], R. Syarif, E. Usai, D. Yu

JHEP03(2019)127

University of California, Davis, Davis, USA
R. Band, C. Brainerd, R. Breedon, D. Burns, M. Calderon De La Barca Sanchez, M. Chertok, J. Conway, R. Conway, P.T. Cox, R. Erbacher, C. Flores, G. Funk, W. Ko, O. Kukral, R. Lander, M. Mulhearn, D. Pellett, J. Pilot, S. Shalhout, M. Shi, D. Stolp, D. Taylor, K. Tos, M. Tripathi, Z. Wang, F. Zhang

University of California, Los Angeles, USA
M. Bachtis, C. Bravo, R. Cousins, A. Dasgupta, A. Florent, J. Hauser, M. Ignatenko, N. Mccoll, S. Regnard, D. Saltzberg, C. Schnaible, V. Valuev

University of California, Riverside, Riverside, USA
E. Bouvier, K. Burt, R. Clare, J.W. Gary, S.M.A. Ghiasi Shirazi, G. Hanson, G. Karapostoli, E. Kennedy, F. Lacroix, O.R. Long, M. Olmedo Negrete, M.I. Paneva, W. Si, L. Wang, H. Wei, S. Wimpenny, B.R. Yates

University of California, San Diego, La Jolla, USA
J.G. Branson, P. Chang, S. Cittolin, M. Derdzinski, R. Gerosa, D. Gilbert, B. Hashemi, A. Holzner, D. Klein, G. Kole, V. Krutelyov, J. Letts, M. Masciovecchio, D. Olivito, S. Padhi, M. Pieri, M. Sani, V. Sharma, S. Simon, M. Tadel, A. Vartak, S. Wasserbaech[67], J. Wood, F. Würthwein, A. Yagil, G. Zevi Della Porta

University of California, Santa Barbara - Department of Physics, Santa Barbara, USA
N. Amin, R. Bhandari, C. Campagnari, M. Citron, V. Dutta, M. Franco Sevilla, L. Gouskos, R. Heller, J. Incandela, H. Mei, A. Ovcharova, H. Qu, J. Richman, D. Stuart, I. Suarez, S. Wang, J. Yoo

California Institute of Technology, Pasadena, USA
D. Anderson, A. Bornheim, J.M. Lawhorn, N. Lu, H.B. Newman, T.Q. Nguyen, M. Spiropulu, J.R. Vlimant, R. Wilkinson, S. Xie, Z. Zhang, R.Y. Zhu

Carnegie Mellon University, Pittsburgh, USA
M.B. Andrews, T. Ferguson, T. Mudholkar, M. Paulini, M. Sun, I. Vorobiev, M. Weinberg

University of Colorado Boulder, Boulder, USA
J.P. Cumalat, W.T. Ford, F. Jensen, A. Johnson, E. MacDonald, T. Mulholland, R. Patel, A. Perloff, K. Stenson, K.A. Ulmer, S.R. Wagner

Cornell University, Ithaca, USA
J. Alexander, J. Chaves, Y. Cheng, J. Chu, A. Datta, K. Mcdermott, N. Mirman, J.R. Patterson, D. Quach, A. Rinkevicius, A. Ryd, L. Skinnari, L. Soffi, S.M. Tan, Z. Tao, J. Thom, J. Tucker, P. Wittich, M. Zientek

Fermi National Accelerator Laboratory, Batavia, USA
S. Abdullin, M. Albrow, M. Alyari, G. Apollinari, A. Apresyan, A. Apyan, S. Banerjee, L.A.T. Bauerdick, A. Beretvas, J. Berryhill, P.C. Bhat, K. Burkett, J.N. Butler, A. Canepa, G.B. Cerati, H.W.K. Cheung, F. Chlebana, M. Cremonesi, J. Duarte, V.D. Elvira, J. Freeman, Z. Gecse, E. Gottschalk, L. Gray, D. Green, S. Grünendahl, O. Gutsche,

JHEP03(2019)127

J. Hanlon, R.M. Harris, S. Hasegawa, J. Hirschauer, Z. Hu, B. Jayatilaka, S. Jindariani, M. Johnson, U. Joshi, B. Klima, M.J. Kortelainen, B. Kreis, S. Lammel, D. Lincoln, R. Lipton, M. Liu, T. Liu, J. Lykken, K. Maeshima, J.M. Marraffino, D. Mason, P. McBride, P. Merkel, S. Mrenna, S. Nahn, V. O'Dell, K. Pedro, C. Pena, O. Prokofyev, G. Rakness, L. Ristori, A. Savoy-Navarro[68], B. Schneider, E. Sexton-Kennedy, A. Soha, W.J. Spalding, L. Spiegel, S. Stoynev, J. Strait, N. Strobbe, L. Taylor, S. Tkaczyk, N.V. Tran, L. Uplegger, E.W. Vaandering, C. Vernieri, M. Verzocchi, R. Vidal, M. Wang, H.A. Weber, A. Whitbeck

University of Florida, Gainesville, USA

D. Acosta, P. Avery, P. Bortignon, D. Bourilkov, A. Brinkerhoff, L. Cadamuro, A. Carnes, D. Curry, R.D. Field, S.V. Gleyzer, B.M. Joshi, J. Konigsberg, A. Korytov, K.H. Lo, P. Ma, K. Matchev, G. Mitselmakher, D. Rosenzweig, K. Shi, D. Sperka, J. Wang, S. Wang, X. Zuo

Florida International University, Miami, USA

Y.R. Joshi, S. Linn

Florida State University, Tallahassee, USA

A. Ackert, T. Adams, A. Askew, S. Hagopian, V. Hagopian, K.F. Johnson, T. Kolberg, G. Martinez, T. Perry, H. Prosper, A. Saha, C. Schiber, R. Yohay

Florida Institute of Technology, Melbourne, USA

M.M. Baarmand, V. Bhopatkar, S. Colafranceschi, M. Hohlmann, D. Noonan, M. Rahmani, T. Roy, F. Yumiceva

University of Illinois at Chicago (UIC), Chicago, USA

M.R. Adams, L. Apanasevich, D. Berry, R.R. Betts, R. Cavanaugh, X. Chen, S. Dittmer, O. Evdokimov, C.E. Gerber, D.A. Hangal, D.J. Hofman, K. Jung, J. Kamin, C. Mills, M.B. Tonjes, N. Varelas, H. Wang, X. Wang, Z. Wu, J. Zhang

The University of Iowa, Iowa City, USA

M. Alhusseini, B. Bilki[69], W. Clarida, K. Dilsiz[70], S. Durgut, R.P. Gandrajula, M. Haytmyradov, V. Khristenko, J.-P. Merlo, A. Mestvirishvili, A. Moeller, J. Nachtman, H. Ogul[71], Y. Onel, F. Ozok[72], A. Penzo, C. Snyder, E. Tiras, J. Wetzel

Johns Hopkins University, Baltimore, USA

B. Blumenfeld, A. Cocoros, N. Eminizer, D. Fehling, L. Feng, A.V. Gritsan, W.T. Hung, P. Maksimovic, J. Roskes, U. Sarica, M. Swartz, M. Xiao, C. You

The University of Kansas, Lawrence, USA

A. Al-bataineh, P. Baringer, A. Bean, S. Boren, J. Bowen, A. Bylinkin, J. Castle, S. Khalil, A. Kropivnitskaya, D. Majumder, W. Mcbrayer, M. Murray, C. Rogan, S. Sanders, E. Schmitz, J.D. Tapia Takaki, Q. Wang

Kansas State University, Manhattan, USA

S. Duric, A. Ivanov, K. Kaadze, D. Kim, Y. Maravin, D.R. Mendis, T. Mitchell, A. Modak, A. Mohammadi

Lawrence Livermore National Laboratory, Livermore, USA

F. Rebassoo, D. Wright

JHEP03(2019)127

University of Maryland, College Park, USA

A. Baden, O. Baron, A. Belloni, S.C. Eno, Y. Feng, C. Ferraioli, N.J. Hadley, S. Jabeen, G.Y. Jeng, R.G. Kellogg, J. Kunkle, A.C. Mignerey, S. Nabili, F. Ricci-Tam, M. Seidel, Y.H. Shin, A. Skuja, S.C. Tonwar, K. Wong

Massachusetts Institute of Technology, Cambridge, USA

D. Abercrombie, B. Allen, V. Azzolini, A. Baty, G. Bauer, R. Bi, S. Brandt, W. Busza, I.A. Cali, M. D'Alfonso, Z. Demiragli, G. Gomez Ceballos, M. Goncharov, P. Harris, D. Hsu, M. Hu, Y. Iiyama, G.M. Innocenti, M. Klute, D. Kovalskyi, Y.-J. Lee, P.D. Luckey, B. Maier, A.C. Marini, C. Mcginn, C. Mironov, S. Narayanan, X. Niu, C. Paus, C. Roland, G. Roland, Z. Shi, G.S.F. Stephans, K. Sumorok, K. Tatar, D. Velicanu, J. Wang, T.W. Wang, B. Wyslouch

University of Minnesota, Minneapolis, USA

A.C. Benvenuti[†], R.M. Chatterjee, A. Evans, P. Hansen, J. Hiltbrand, Sh. Jain, S. Kalafut, M. Krohn, Y. Kubota, Z. Lesko, J. Mans, N. Ruckstuhl, R. Rusack, M.A. Wadud

University of Mississippi, Oxford, USA

J.G. Acosta, S. Oliveros

University of Nebraska-Lincoln, Lincoln, USA

E. Avdeeva, K. Bloom, D.R. Claes, C. Fangmeier, F. Golf, R. Gonzalez Suarez, R. Kamalieddin, I. Kravchenko, J. Monroy, J.E. Siado, G.R. Snow, B. Stieger

State University of New York at Buffalo, Buffalo, USA

A. Godshalk, C. Harrington, I. Iashvili, A. Kharchilava, C. Mclean, D. Nguyen, A. Parker, S. Rappoccio, B. Roozbahani

Northeastern University, Boston, USA

G. Alverson, E. Barberis, C. Freer, Y. Haddad, A. Hortiangtham, D.M. Morse, T. Orimoto, T. Wamorkar, B. Wang, A. Wisecarver, D. Wood

Northwestern University, Evanston, USA

S. Bhattacharya, J. Bueghly, O. Charaf, T. Gunter, K.A. Hahn, N. Mucia, N. Odell, M.H. Schmitt, K. Sung, M. Trovato, M. Velasco

University of Notre Dame, Notre Dame, USA

R. Bucci, N. Dev, M. Hildreth, K. Hurtado Anampa, C. Jessop, D.J. Karmgard, N. Kellams, K. Lannon, W. Li, N. Loukas, N. Marinelli, F. Meng, C. Mueller, Y. Musienko[36], M. Planer, A. Reinsvold, R. Ruchti, P. Siddireddy, G. Smith, S. Taroni, M. Wayne, A. Wightman, M. Wolf, A. Woodard

The Ohio State University, Columbus, USA

J. Alimena, L. Antonelli, B. Bylsma, L.S. Durkin, S. Flowers, B. Francis, C. Hill, W. Ji, T.Y. Ling, W. Luo, B.L. Winer

JHEP03(2019)127

Princeton University, Princeton, USA

S. Cooperstein, P. Elmer, J. Hardenbrook, S. Higginbotham, A. Kalogeropoulos, D. Lange, M.T. Lucchini, J. Luo, D. Marlow, K. Mei, I. Ojalvo, J. Olsen, C. Palmer, P. Piroué, J. Salfeld-Nebgen, D. Stickland, C. Tully, Z. Wang

University of Puerto Rico, Mayaguez, USA

S. Malik, S. Norberg

Purdue University, West Lafayette, USA

A. Barker, V.E. Barnes, S. Das, L. Gutay, M. Jones, A.W. Jung, A. Khatiwada, B. Mahakud, D.H. Miller, N. Neumeister, C.C. Peng, S. Piperov, H. Qiu, J.F. Schulte, J. Sun, F. Wang, R. Xiao, W. Xie

Purdue University Northwest, Hammond, USA

T. Cheng, J. Dolen, N. Parashar

Rice University, Houston, USA

Z. Chen, K.M. Ecklund, S. Freed, F.J.M. Geurts, M. Kilpatrick, W. Li, B.P. Padley, R. Redjimi, J. Roberts, J. Rorie, W. Shi, Z. Tu, A. Zhang

University of Rochester, Rochester, USA

A. Bodek, P. de Barbaro, R. Demina, Y.t. Duh, J.L. Dulemba, C. Fallon, T. Ferbel, M. Galanti, A. Garcia-Bellido, J. Han, O. Hindrichs, A. Khukhunaishvili, E. Ranken, P. Tan, R. Taus

Rutgers, The State University of New Jersey, Piscataway, USA

J.P. Chou, Y. Gershtein, E. Halkiadakis, A. Hart, M. Heindl, E. Hughes, S. Kaplan, R. Kunnawalkam Elayavalli, S. Kyriacou, I. Laflotte, A. Lath, R. Montalvo, K. Nash, M. Osherson, H. Saka, S. Salur, S. Schnetzer, D. Sheffield, S. Somalwar, R. Stone, S. Thomas, P. Thomassen, M. Walker

University of Tennessee, Knoxville, USA

A.G. Delannoy, J. Heideman, G. Riley, S. Spanier

Texas A&M University, College Station, USA

O. Bouhali[73], A. Celik, M. Dalchenko, M. De Mattia, A. Delgado, S. Dildick, R. Eusebi, J. Gilmore, T. Huang, T. Kamon[74], S. Luo, D. Marley, R. Mueller, D. Overton, L. Perniè, D. Rathjens, A. Safonov

Texas Tech University, Lubbock, USA

N. Akchurin, J. Damgov, F. De Guio, P.R. Dudero, S. Kunori, K. Lamichhane, S.W. Lee, T. Mengke, S. Muthumuni, T. Peltola, S. Undleeb, I. Volobouev, Z. Wang

Vanderbilt University, Nashville, USA

S. Greene, A. Gurrola, R. Janjam, W. Johns, C. Maguire, A. Melo, H. Ni, K. Padeken, F. Romeo, J.D. Ruiz Alvarez, P. Sheldon, S. Tuo, J. Velkovska, M. Verweij, Q. Xu

JHEP03(2019)127

University of Virginia, Charlottesville, USA

M.W. Arenton, P. Barria, B. Cox, R. Hirosky, M. Joyce, A. Ledovskoy, H. Li, C. Neu, T. Sinthuprasith, Y. Wang, E. Wolfe, F. Xia

Wayne State University, Detroit, USA

R. Harr, P.E. Karchin, N. Poudyal, J. Sturdy, P. Thapa, S. Zaleski

University of Wisconsin - Madison, Madison, WI, USA

J. Buchanan, C. Caillol, D. Carlsmith, S. Dasu, I. De Bruyn, L. Dodd, B. Gomber, M. Grothe, M. Herndon, A. Hervé, U. Hussain, P. Klabbers, A. Lanaro, K. Long, R. Loveless, T. Ruggles, A. Savin, V. Sharma, N. Smith, W.H. Smith, N. Woods

†: Deceased
1: Also at Vienna University of Technology, Vienna, Austria
2: Also at IRFU, CEA, Université Paris-Saclay, Gif-sur-Yvette, France
3: Also at Universidade Estadual de Campinas, Campinas, Brazil
4: Also at Federal University of Rio Grande do Sul, Porto Alegre, Brazil
5: Also at Université Libre de Bruxelles, Bruxelles, Belgium
6: Also at University of Chinese Academy of Sciences, Beijing, China
7: Also at Institute for Theoretical and Experimental Physics, Moscow, Russia
8: Also at Joint Institute for Nuclear Research, Dubna, Russia
9: Also at Fayoum University, El-Fayoum, Egypt
10: Now at British University in Egypt, Cairo, Egypt
11: Now at Ain Shams University, Cairo, Egypt
12: Also at Department of Physics, King Abdulaziz University, Jeddah, Saudi Arabia
13: Also at Université de Haute Alsace, Mulhouse, France
14: Also at Skobeltsyn Institute of Nuclear Physics, Lomonosov Moscow State University, Moscow, Russia
15: Also at Tbilisi State University, Tbilisi, Georgia
16: Also at CERN, European Organization for Nuclear Research, Geneva, Switzerland
17: Also at RWTH Aachen University, III. Physikalisches Institut A, Aachen, Germany
18: Also at University of Hamburg, Hamburg, Germany
19: Also at Brandenburg University of Technology, Cottbus, Germany
20: Also at Institute of Physics, University of Debrecen, Debrecen, Hungary
21: Also at Institute of Nuclear Research ATOMKI, Debrecen, Hungary
22: Also at MTA-ELTE Lendület CMS Particle and Nuclear Physics Group, Eötvös Loránd University, Budapest, Hungary
23: Also at Indian Institute of Technology Bhubaneswar, Bhubaneswar, India
24: Also at Institute of Physics, Bhubaneswar, India
25: Also at Shoolini University, Solan, India
26: Also at University of Visva-Bharati, Santiniketan, India
27: Also at Isfahan University of Technology, Isfahan, Iran
28: Also at Plasma Physics Research Center, Science and Research Branch, Islamic Azad University, Tehran, Iran
29: Also at Università degli Studi di Siena, Siena, Italy
30: Also at Scuola Normale e Sezione dell'INFN, Pisa, Italy
31: Also at Kyunghee University, Seoul, Korea
32: Also at International Islamic University of Malaysia, Kuala Lumpur, Malaysia

JHEP03(2019)127

33: Also at Malaysian Nuclear Agency, MOSTI, Kajang, Malaysia
34: Also at Consejo Nacional de Ciencia y Tecnología, Mexico City, Mexico
35: Also at Warsaw University of Technology, Institute of Electronic Systems, Warsaw, Poland
36: Also at Institute for Nuclear Research, Moscow, Russia
37: Now at National Research Nuclear University 'Moscow Engineering Physics Institute' (MEPhI), Moscow, Russia
38: Also at St. Petersburg State Polytechnical University, St. Petersburg, Russia
39: Also at University of Florida, Gainesville, USA
40: Also at P.N. Lebedev Physical Institute, Moscow, Russia
41: Also at California Institute of Technology, Pasadena, USA
42: Also at Budker Institute of Nuclear Physics, Novosibirsk, Russia
43: Also at Faculty of Physics, University of Belgrade, Belgrade, Serbia
44: Also at INFN Sezione di Pavia [a], Università di Pavia [b], Pavia, Italy
45: Also at University of Belgrade, Faculty of Physics and Vinca Institute of Nuclear Sciences, Belgrade, Serbia
46: Also at National and Kapodistrian University of Athens, Athens, Greece
47: Also at Riga Technical University, Riga, Latvia
48: Also at Universität Zürich, Zurich, Switzerland
49: Also at Stefan Meyer Institute for Subatomic Physics (SMI), Vienna, Austria
50: Also at Gaziosmanpasa University, Tokat, Turkey
51: Also at Adiyaman University, Adiyaman, Turkey
52: Also at Istanbul Aydin University, Istanbul, Turkey
53: Also at Mersin University, Mersin, Turkey
54: Also at Piri Reis University, Istanbul, Turkey
55: Also at Ozyegin University, Istanbul, Turkey
56: Also at Izmir Institute of Technology, Izmir, Turkey
57: Also at Marmara University, Istanbul, Turkey
58: Also at Kafkas University, Kars, Turkey
59: Also at Istanbul University, Faculty of Science, Istanbul, Turkey
60: Also at Istanbul Bilgi University, Istanbul, Turkey
61: Also at Hacettepe University, Ankara, Turkey
62: Also at Rutherford Appleton Laboratory, Didcot, United Kingdom
63: Also at School of Physics and Astronomy, University of Southampton, Southampton, United Kingdom
64: Also at Monash University, Faculty of Science, Clayton, Australia
65: Also at Bethel University, St. Paul, USA
66: Also at Karamanoğlu Mehmetbey University, Karaman, Turkey
67: Also at Utah Valley University, Orem, USA
68: Also at Purdue University, West Lafayette, USA
69: Also at Beykent University, Istanbul, Turkey
70: Also at Bingol University, Bingol, Turkey
71: Also at Sinop University, Sinop, Turkey
72: Also at Mimar Sinan University, Istanbul, Istanbul, Turkey
73: Also at Texas A&M University at Qatar, Doha, Qatar
74: Also at Kyungpook National University, Daegu, Korea

JHEP03(2019)127